Synchrotron Radiation Facilities and Frequency Map Analysis

Workshop in Honor of Jacques Laskar, April 28-30, 2015
Astronomy and Dynamics Workshop

$$F^T : \mathbb{R}^2 \rightarrow \mathbb{R}^2$$
$$(x,\, y) \mapsto (\nu_x,\, \nu_y)$$

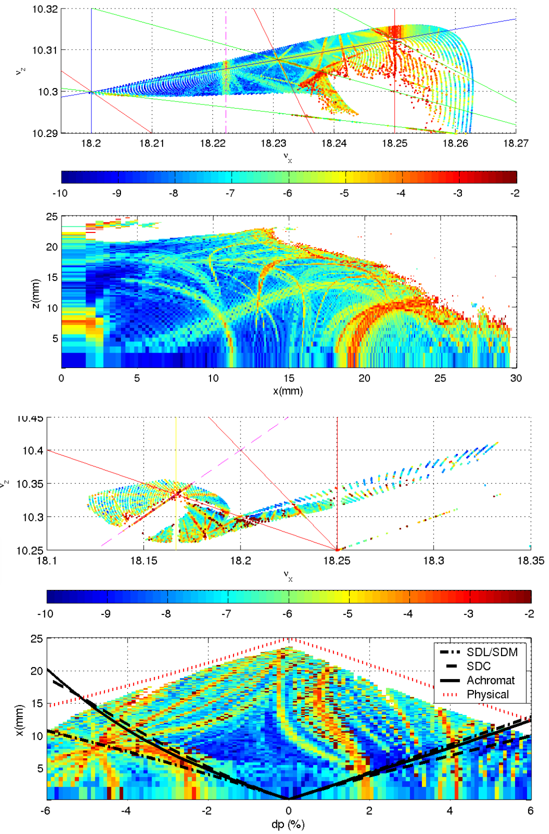

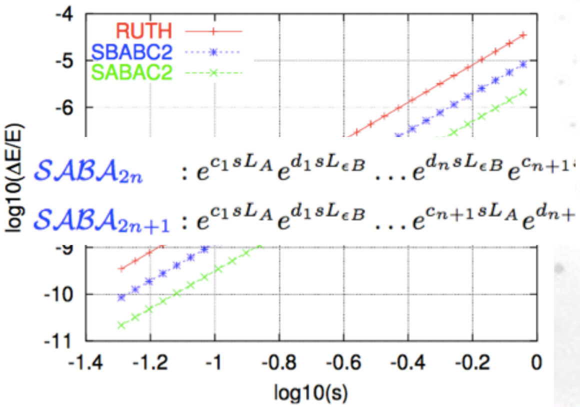

Laurent S. Nadolski
Accelerator Coordinator
Synchrotron SOLEIL, France
www.synchrotron-soleil.fr

Meeting with Jacques 18 years ago …

Simplified model for checking the main results on the rotation axis of Earth over 20 millions years and graphic representation. Report Technical, Bureau des Longitudes, Paris, France, 1997

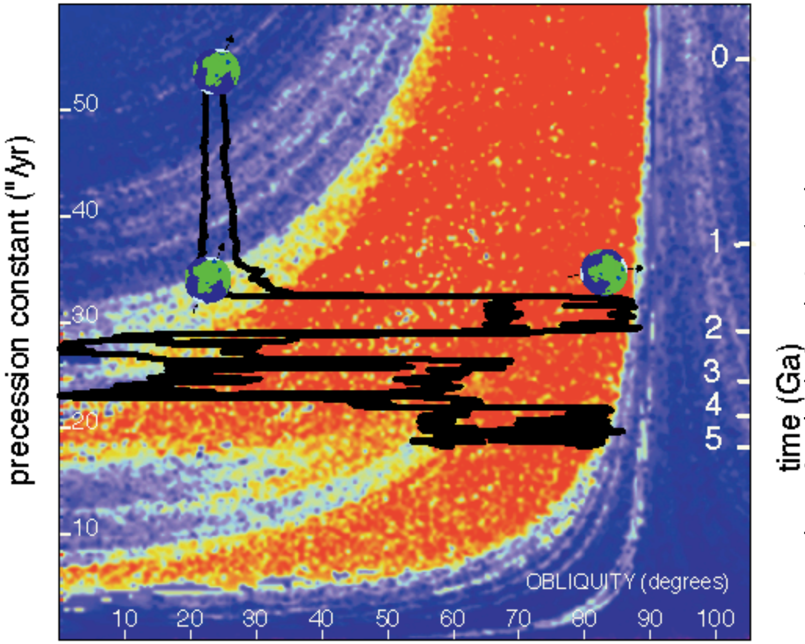

Evolution of the Earth's obliquity for 5 Gyr in the future. In the background, the color gives the stability of the spin axis of the Earth. Blue corresponds to stable motion, and red to highly chaotic behavior. The time from nom is given in Gyr on the left axis, and the Earth obliquity (inclination of the equator on the orbital plane of the Earth) is on the horizontal axis. At present, the average obliquity of the Earth is 23.25 degrees, and the obliquity oscillates around this value with 40 kyr periods and 1.3 degrees amplitude. The black curves represent the limits of this oscillation. As the times goes, du to tidal interactions in the Earth-Moon system, the Earth rotation slows down and the Moon goes away at 3.8 cm/year. The torque exerted on the equatorial bulge of the Earth thus diminish, and the precession frequency of the Earth spin axis (on the left axis of the figure) decreases. After about 1.5 Gyr, the precession period of the Earth becomes comparable to the precession periods of the orbital plane of the Earth, due to planetary perturbations. The Earth then enters a large chaotic zone (in red) and the spin axis wanders chaotically between 0 and more than 85 degrees. As the motion is chaotic, a small difference will lead to a different solution, but the general behavior depicted here will remain the same, and there is no possibility for the Earth to avoid entering into the zone of strong chaotic motion (in red) (Laskar et al., 1993, Laskar and Robutel, 1993, Neron de Surgy and Laskar, 1997).

Contents

- Introduction to Light Sources
- Modeling of circular accelerators and Symplectic integrators
- Frequency Map Analysis (FMA)
  - Global vision of the dynamics
  - a standard tool of the accelerator community
- Use of FMA for today and tomorrow accelerators
- Laskar's Legacy

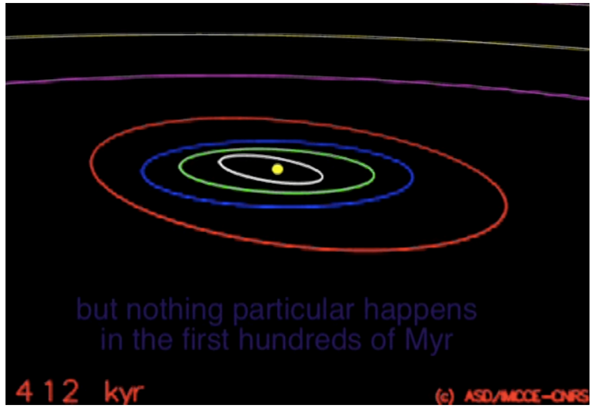

Millions of **years**

Millions of **turns**

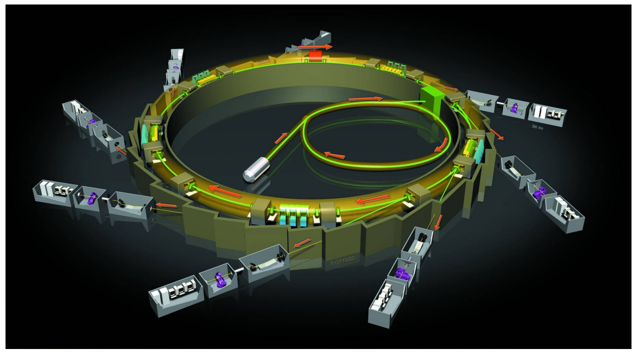

Introduction and main concepts

SYNCHROTRON RADIATION FACILITIES OR LIGHT SOURCES

Brief History

Synchrotron Radiation (SR) Discovery

- It all started in 1254 when the Crab Nebula exploded and became visible for two weeks even in daylight.
- 1879 Maxwell's equations
- 1886 Heinrich Hertz demonstrated such waves.
- First observed in 1947 in GE Synchrotron by Edler et al.

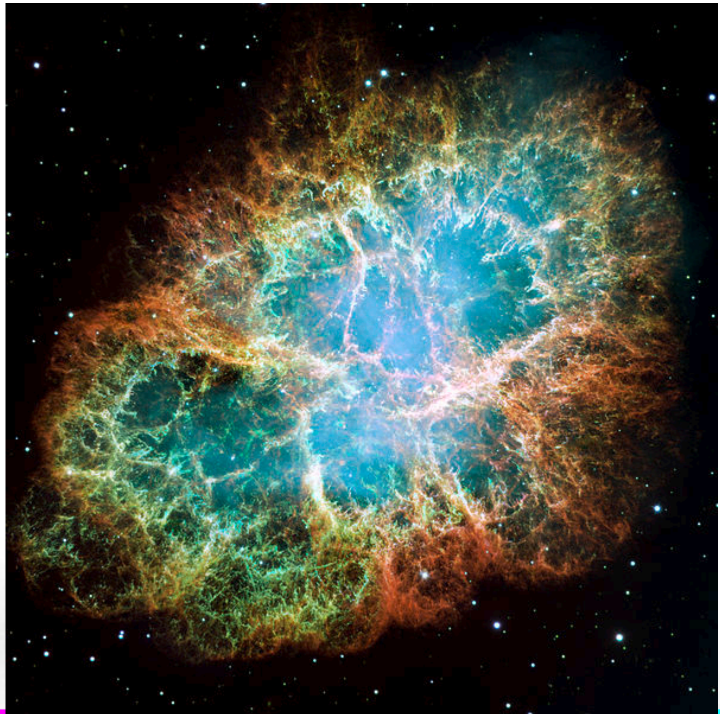

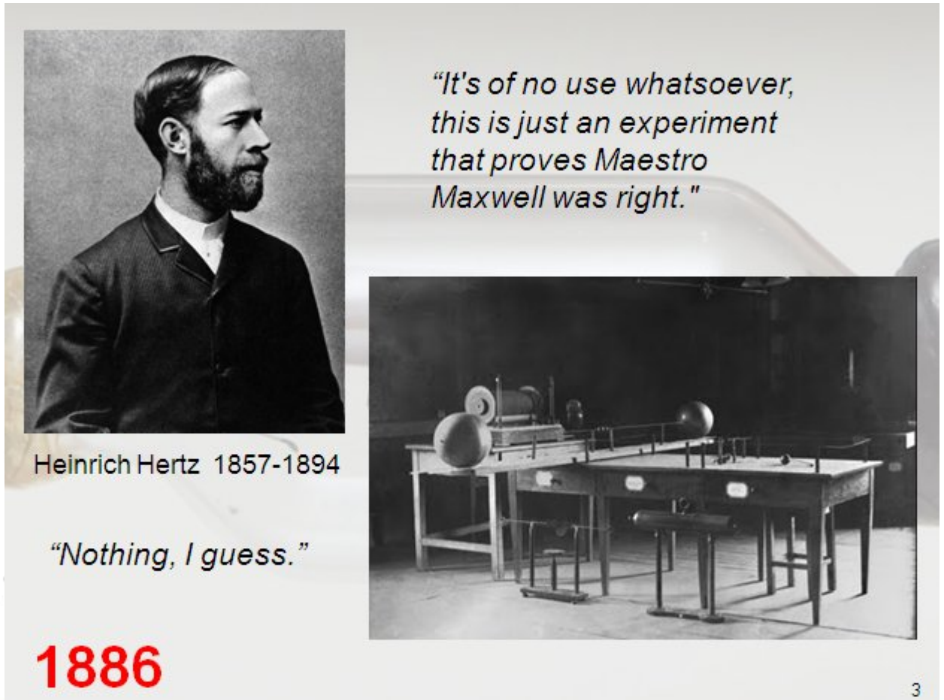

First visible observation

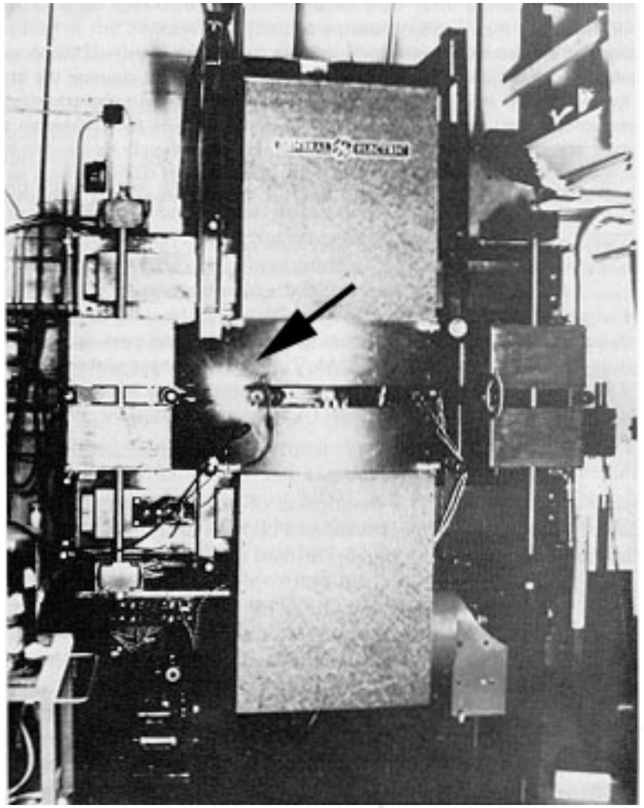

General Electric Research Laboratory, Schenectady, NY
Bluish white spot observed by F. Haber on April 24th, 1947

F.R. Elder A.M. Gurewitsch E.E. Charlton

R.V. Langmuir

H.C. Pollock

Yellow around 40 MeV
Red around 30 MeV
Disappeared below 20 MeV

Visible radiation was observed for the first time at the 70 MeV synchrotron built in 1946.

Since then this radiation is called synchrotron radiation.

Accelerator scheme: SOLEIL example

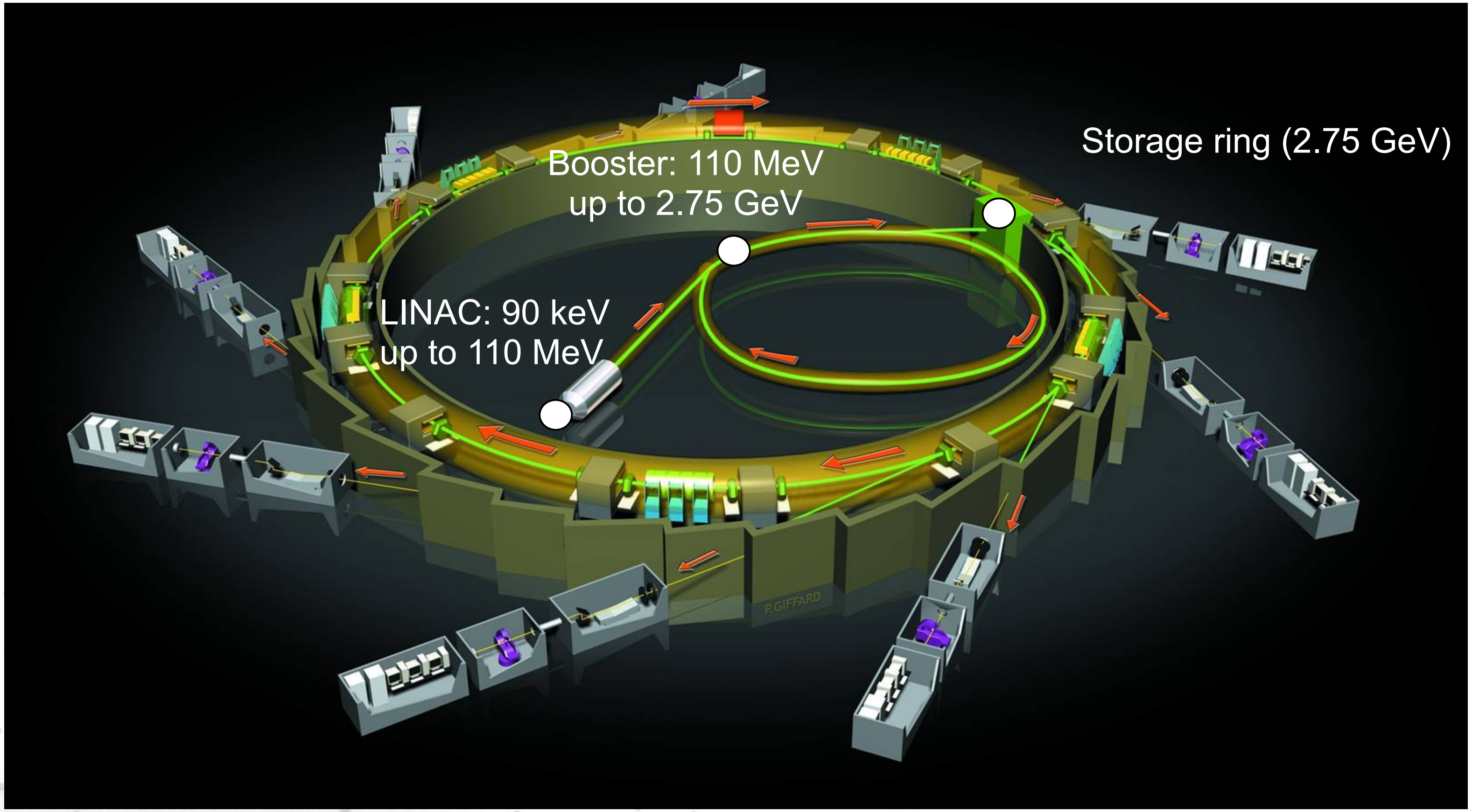

Storage ring: 354 m long circumference, γ = 5382, ρ = 5.36 m, B = 1.71 T

Magnets for guiding and focusing the electron beam

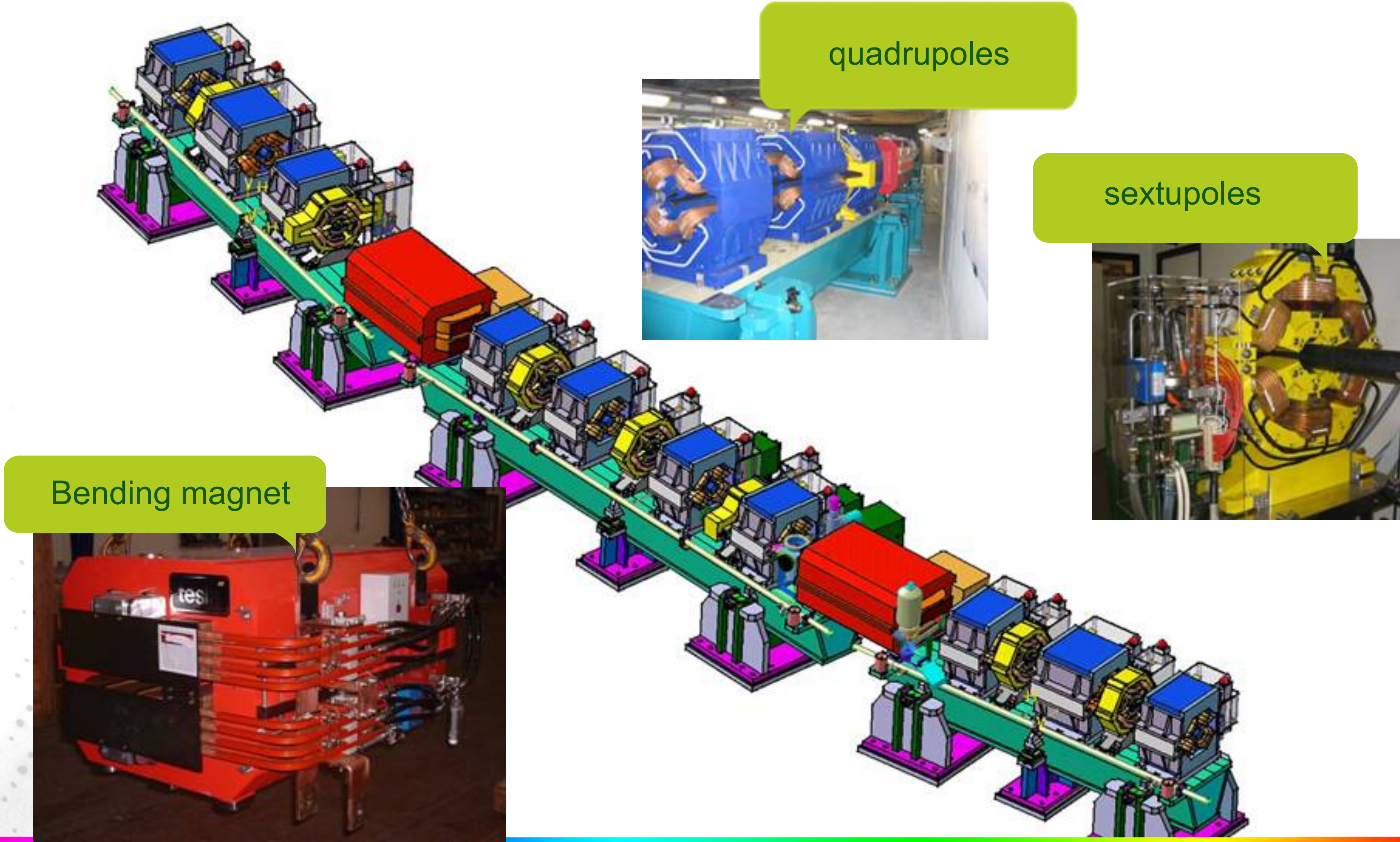

SOLEIL girder equipped with magnets

Ultra relativistic electrons can be deviated by the constant magnetic field of bending magnets in which their trajectory is an arc of circle

Due to the bending of their trajectory, they are slowed down by their self field and lose energy

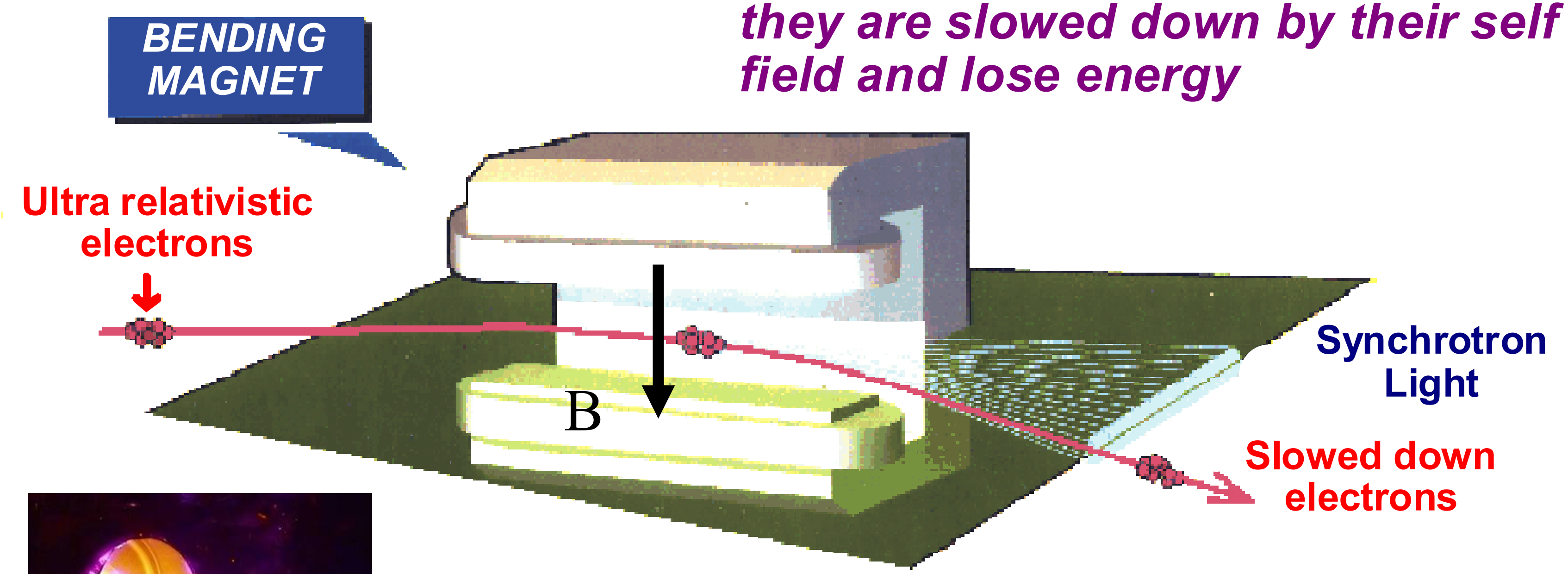

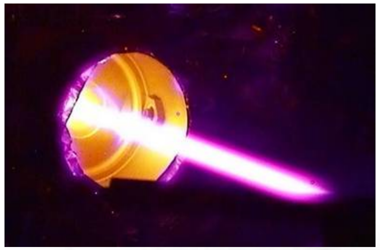

They emit photons in a direction tangent to their trajectory
This is synchrotron radiation

Such conditions are met in electron storage rings

$$P_{rad} = \frac{2 r_e c}{3 m_0 c^2} \gamma^2 \left(\frac{dp}{dt} \right)^2$$

Angular distribution of synchrotron radiation

- The axially-symmetric radiation distribution in the moving frame K' (a.) transforms into a sharply forward peaked distribution in the laboratory frame (b.), with a half opening-angle $\theta = 1/\gamma$.

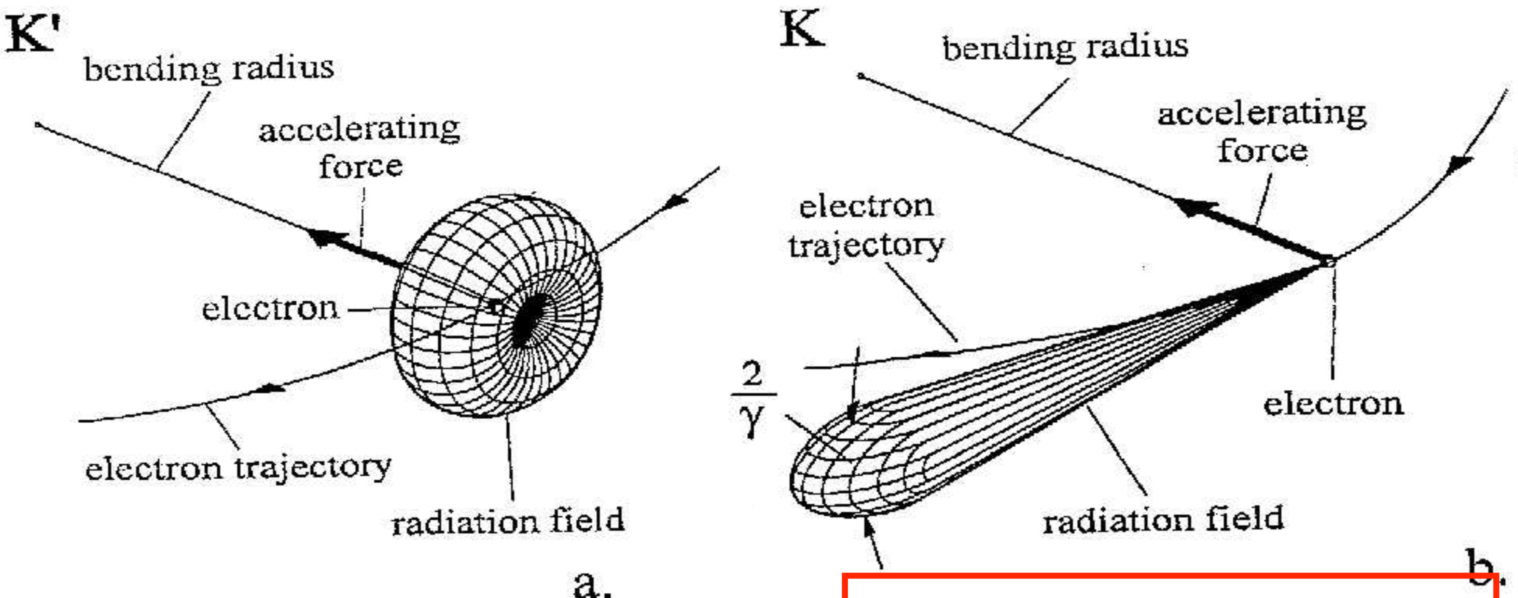

Moving frame
Donut-shape radiation pattern

Laboratory frame
Relativistic case
Forward radiation pattern

For E = 2.75 GeV: γ = 5382 then θ = 0.186 mrad = 0.01°

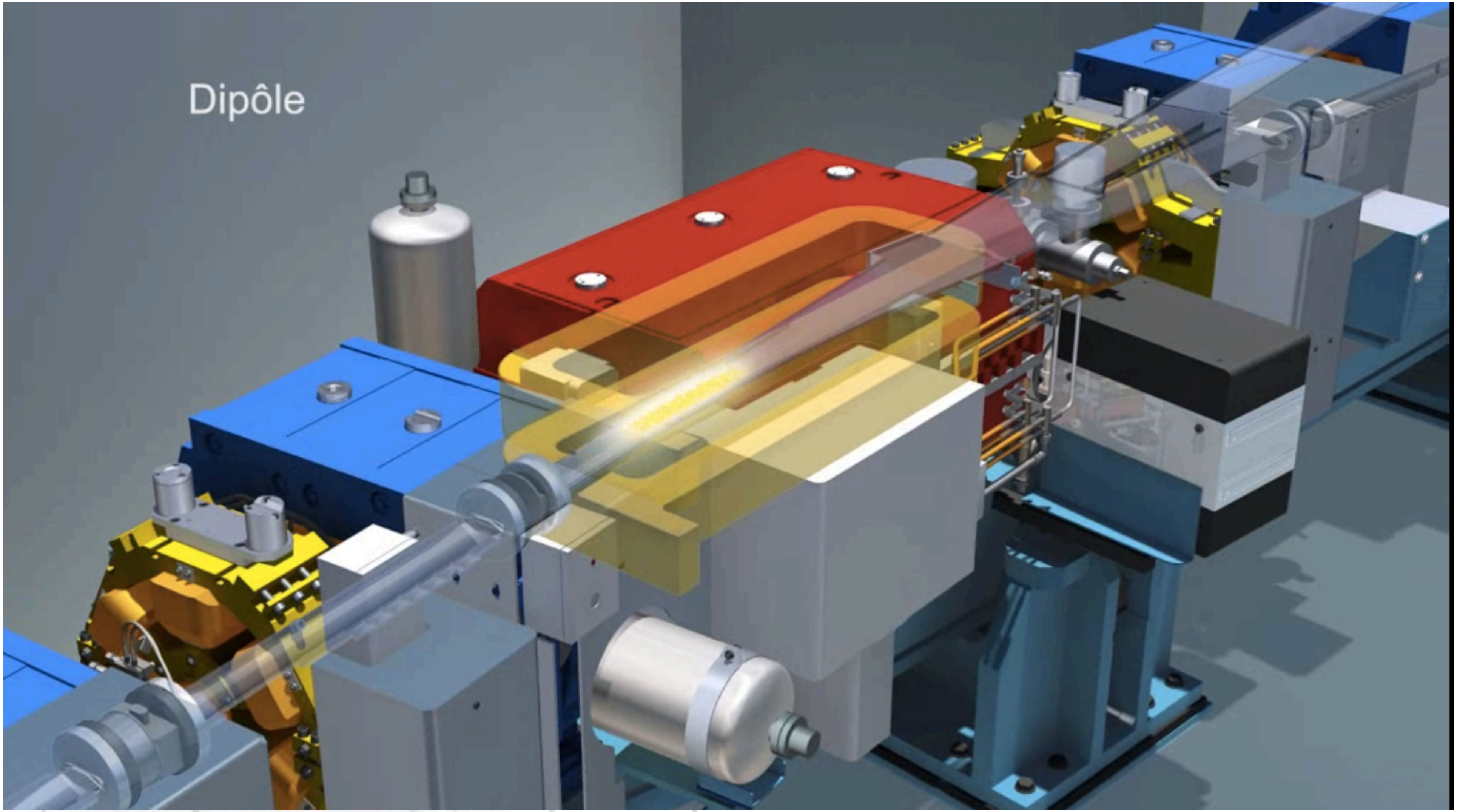
Dipôle

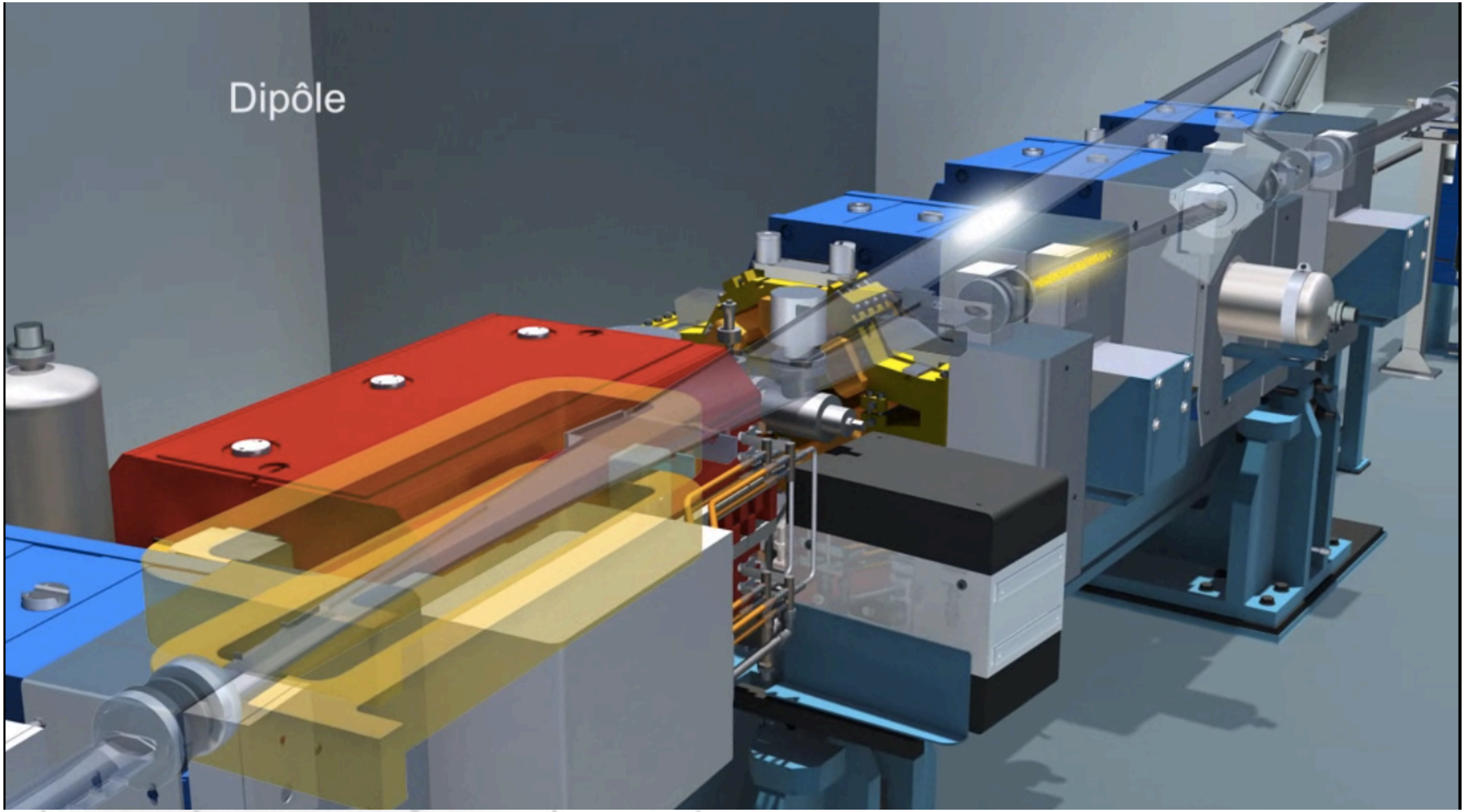
Dipôle

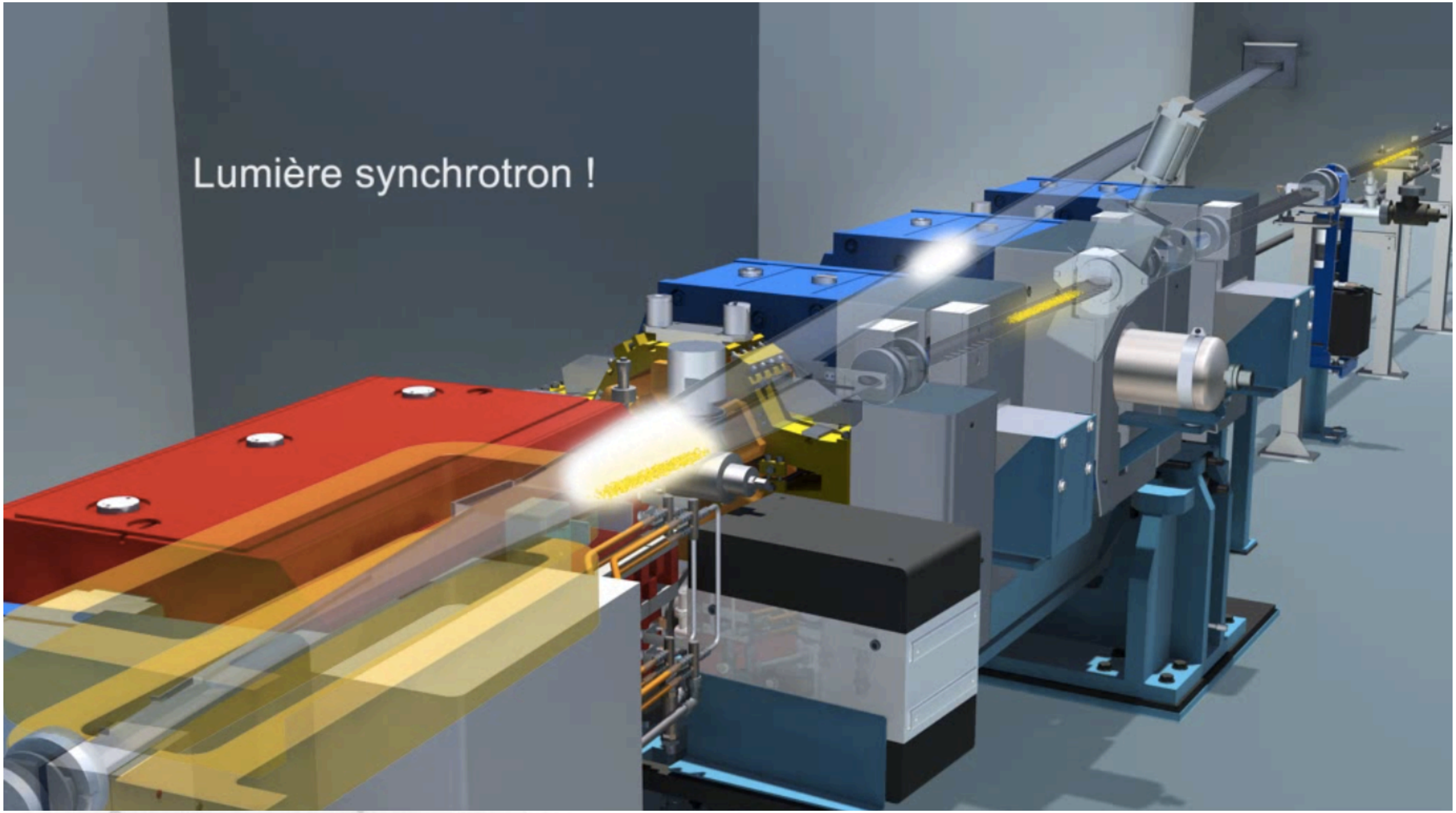
Lumière synchrotron !

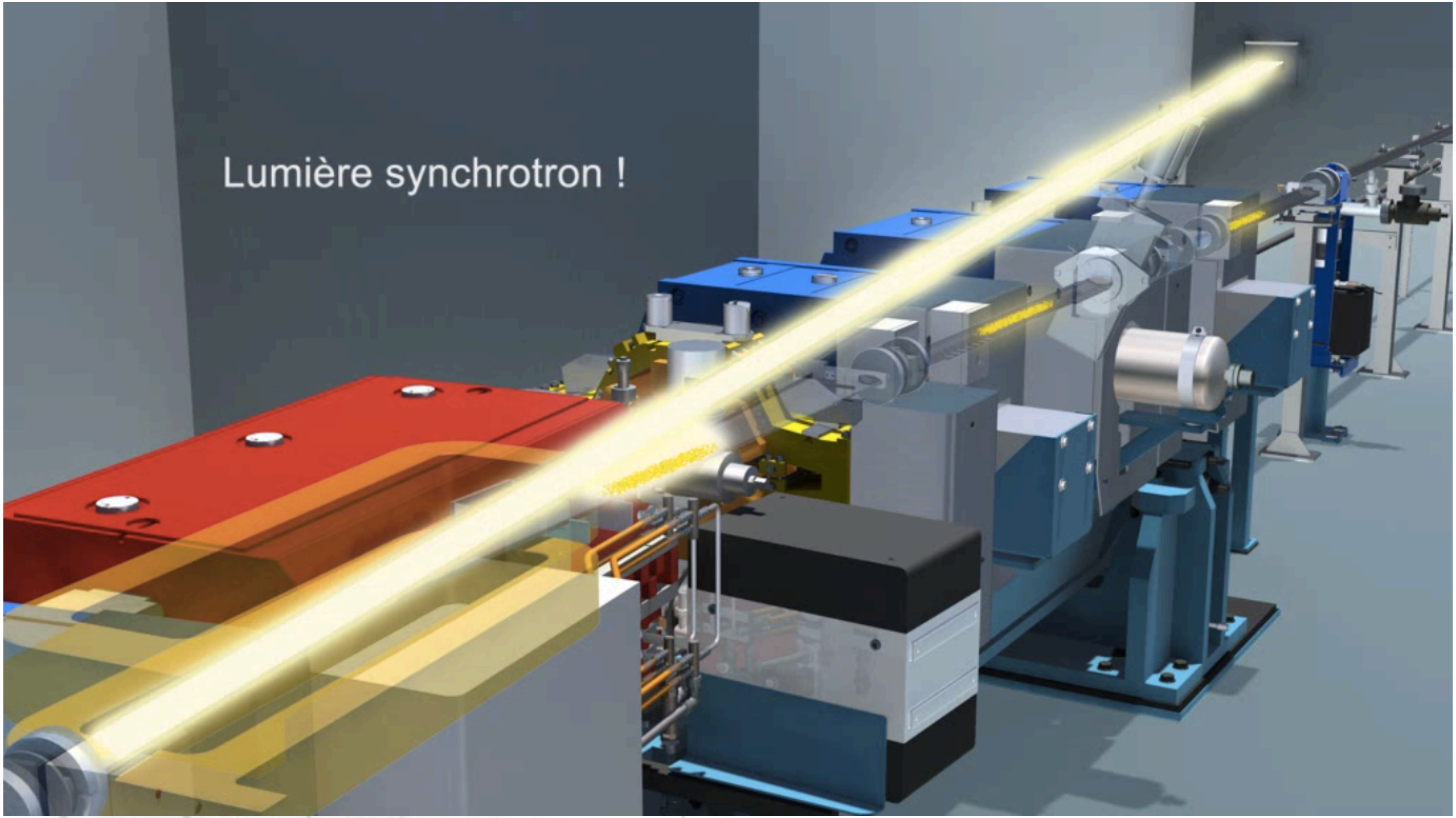
Lumière synchrotron !

Insertion devices

$$\lambda \approx \frac{\lambda_0}{2\gamma^2} \cdot \left(1 + \gamma^2 \theta^2\right)$$

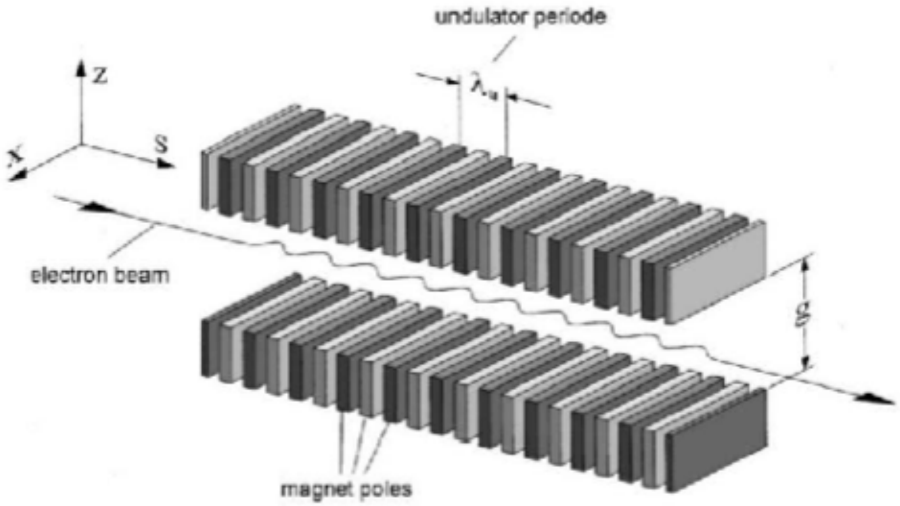

The γ factor is large: 5382 for E = 2.75 GeV: λ_0=20 mm → λ = 3.45 Å

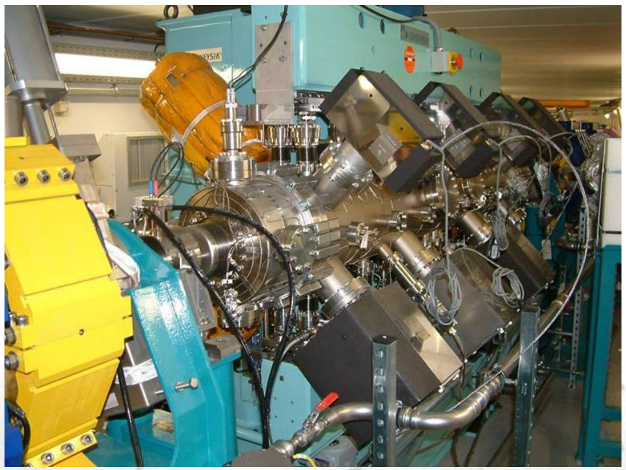

In-vacuum Undulator U20

Period 20 mm
3 – 18 keV

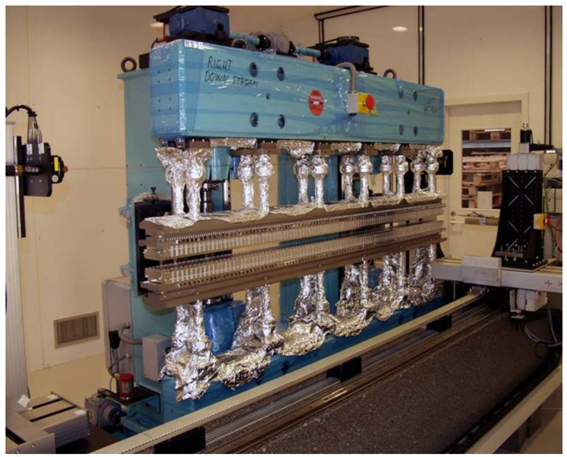

Light properties

Brilliant - many orders of magnitude brighter than conventional sources, enabling quick experiments on small size samples.

Collimated - beam can be focused down to less than a micron (10^{-6} m) across, enabling chemical speciation to be mapped.

Polarized - linear polarization, minimizes background scattering, improves sensitivity

Pulsed - electron bunches produce short light pulses, enabling process kinetics to be followed.

Broadband spectrum - from infrared to hard X-rays, optical devices select and scan the light's energy.

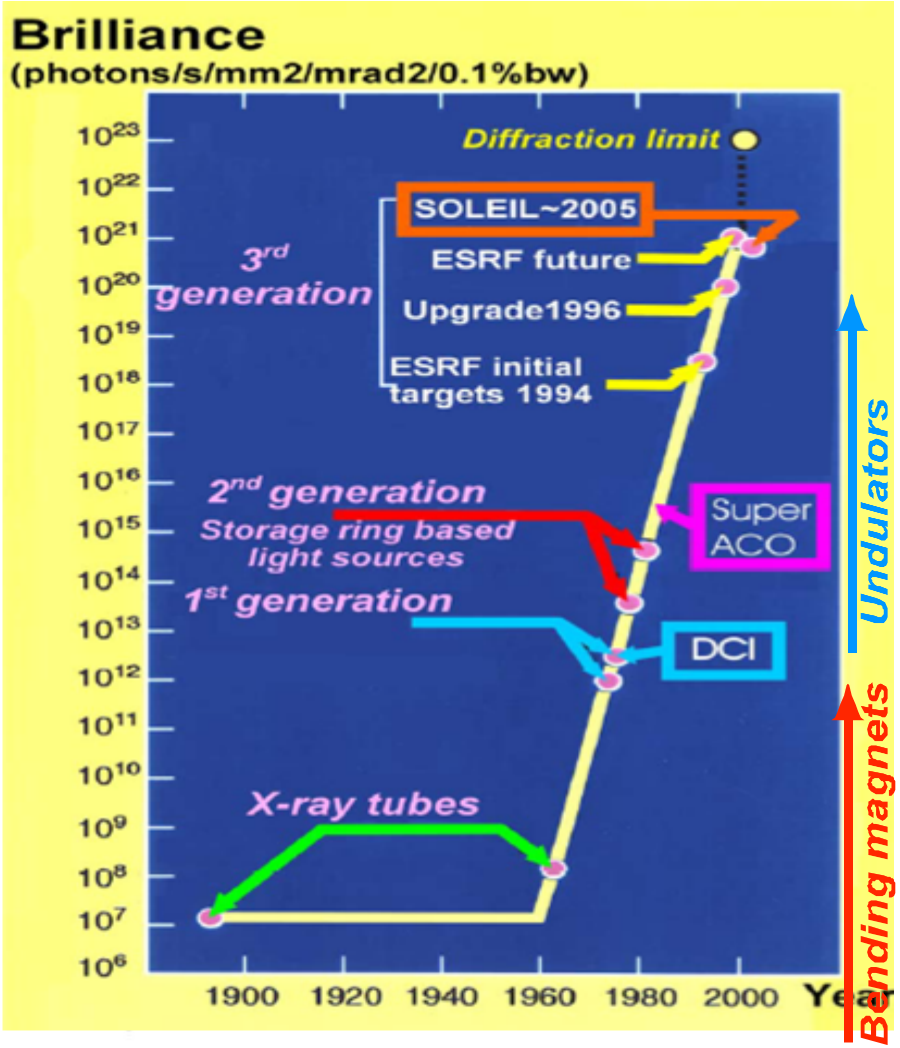

Main application fields

Visualization of polluting agents

Knowledge of structure of the matter

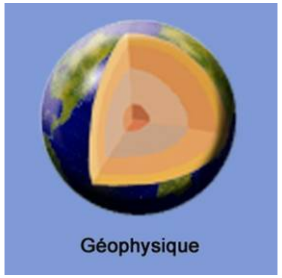

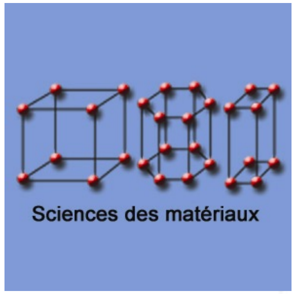

Exploration of (the) matters and knowledge of their properties

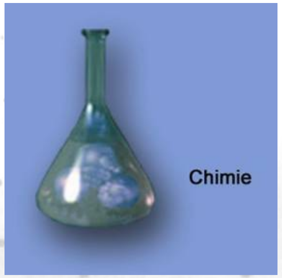

Foodstuff preservation

New material processing

Research of new drugs, osseous tissue imaging, DNA study…

Today light sources' chart

Nearly 80 facilities producing synchrotron light

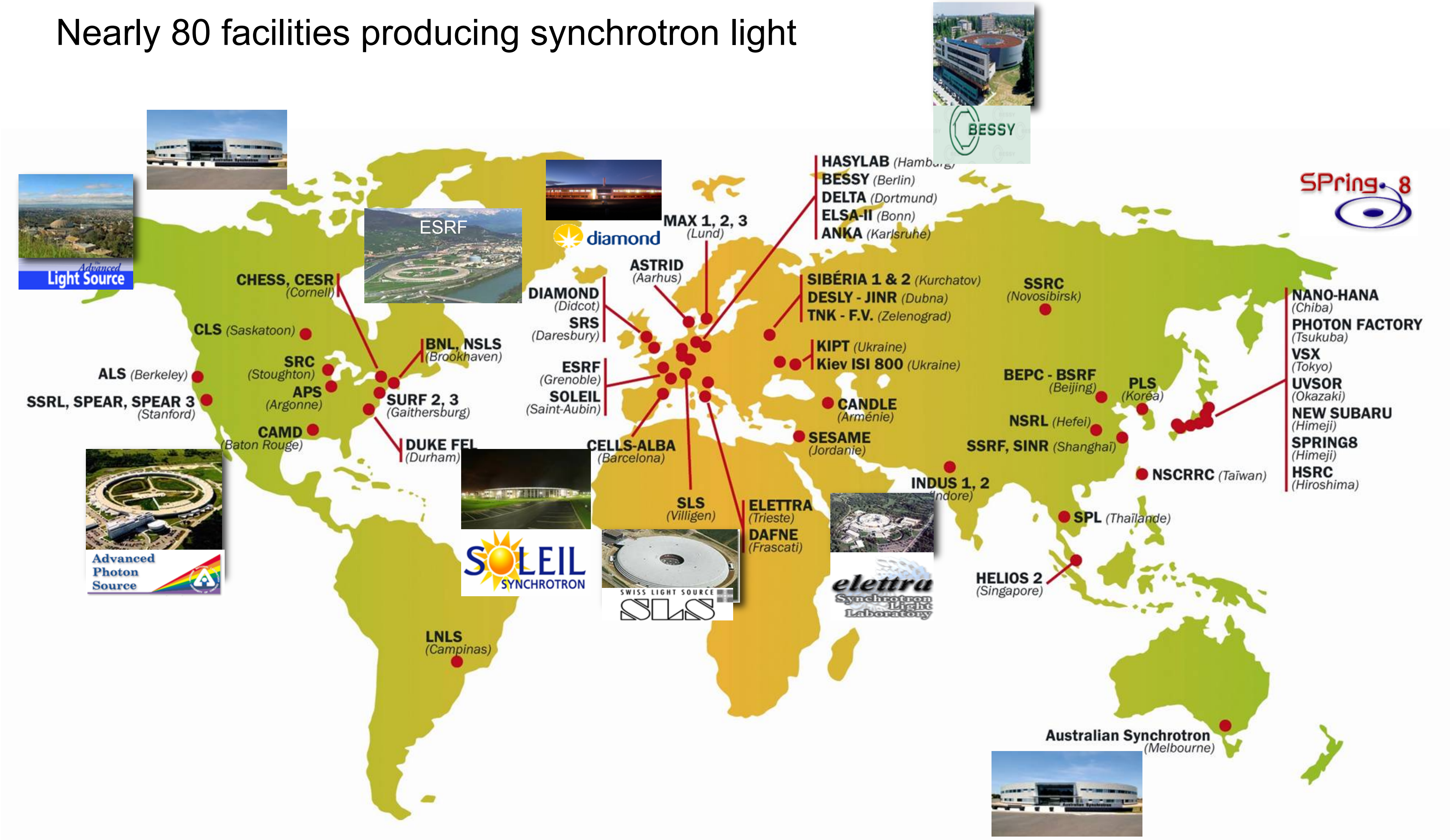

Hamiltonian system

Symplectic integrators

MODELING OF PARTICLE ACCELERATORS

A brief History of Frequency Map Analysis (FMA)

- For many centuries, the motion of planets in the Solar System was considered as **perfectly regular.**
- In 1988, J. Laskar (Paris Observatory) published evidence of chaotic motion in the Solar Systems using a new method called Frequency Map Analysis (FMA).
- FMA was successively applied to the study of dynamics systems such as (short list)
  - Stability of Earth Obliquity and climate stabilization (Laskar, Robutel, 1993)
  - Standard application (Laskar, Floeschlé, Celleti, 1992, Laskar and Carletti 2000)
  - Galactic Dynamics (Papaphilippou et Laskar, 1996 and 1998)
  - Accelerator beam dynamics: lepton and hadron storage rings (Dumas, Laskar, 1993, Laskar, Robin, 1996, Papaphilippou, 1999, ...)

Particle Accelerators: transverse beam dynamics and stability

Introduction: Studying Nonlinear Dynamics

Nonlinear dynamics

- Complex dynamics
- Resonances
- Tunes shift with amplitudes
- Chaos, instabilities
- Instability thresholds

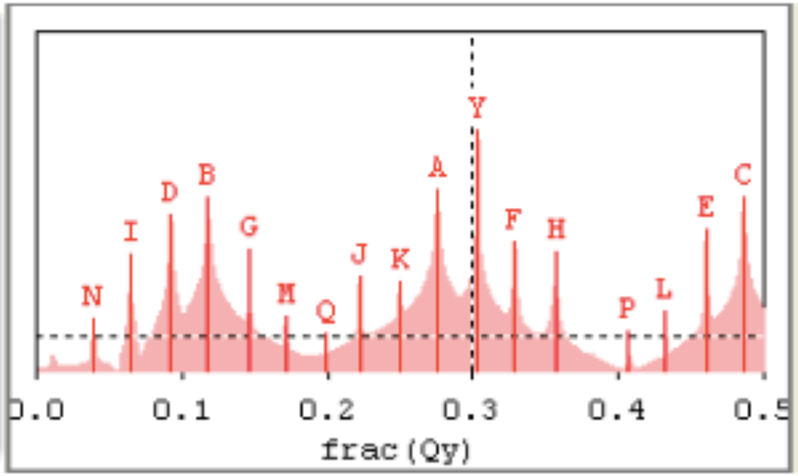

Need of an accurate way to compute frequencies. Fast Fourier Transform (FFT) is an efficient algorithm (Cooley-Tukey, 1965) and a powerful way yet limited. Precision is $1/T$. To get high precision frequencies (tunes), very long integration, many data, or turns are needed.

Local Hamiltonian Approach

- Motion with respect to a reference particle.
- Canonical variables (x, p_x), (y, p_y), (l, δ)
- Time-like variable s

Potential vector $(\hat{A}_x,\ \hat{A}_y,\ \hat{A}_s)$

- Maxwell equations
- Symmetries
- Longitudinal rectangular magnetic profile

$$\mathcal{H} = -(1 + h(s)x)\sqrt{(1+\delta)^2 - (p_x - e\hat{A}_x)^2 - (p_y - e\hat{A}_y)^2} - e\hat{A}_s + \delta + 1 \quad (7)$$

$$-e\hat{A}_s(x, y) = \mathrm{Re}\left(\sum_{n=1}^{\infty} \frac{b_n + ja_n}{n}(x + jy)^n\right) \quad (8)$$

with $h(s) = 1/\rho(s)$.

a_n and b_n coefficients: skew and normal 2n–poles

Tracking codes

- **Long term tracking based on symplectic integrators**
  - Implicit or explicit schemes
- **Popularized by Ruth and Forest 1983-1990, use of Lie Algebra (Neri, 1988), Yoshida techniques (1990), Channel and Scovel (1990), Mclachlan (1995), Sanz-Serna (1998), Laskar integrators (2001)**
  - Preserves energy, bounded errors,
  - Phase stability
  - Used by MADX/PTC, Tracy, OPA, LEGO, ELEGANT, etc

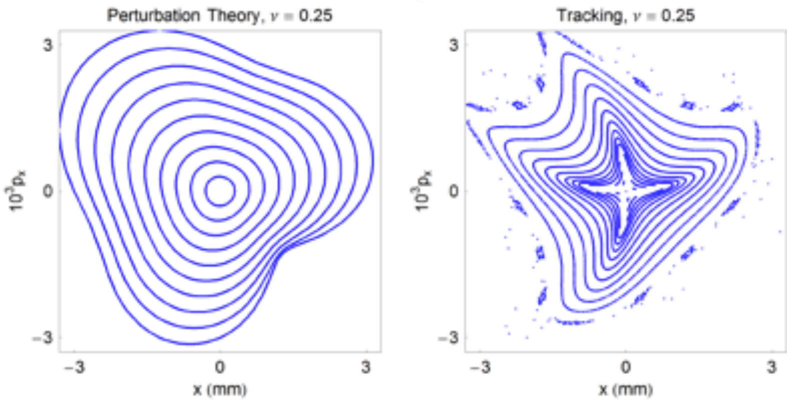

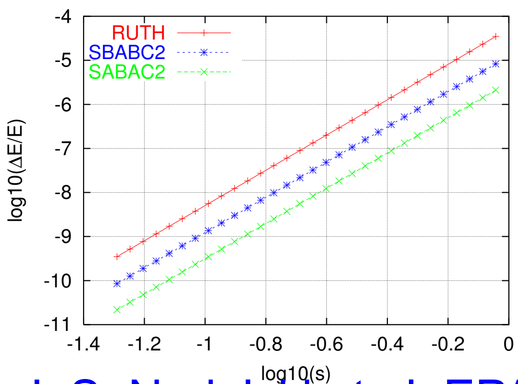

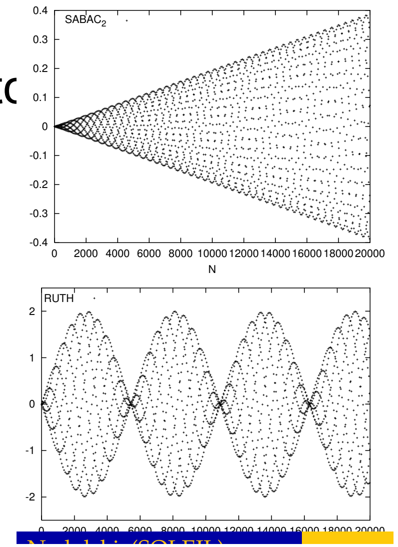

L S. Nadolski et al. EPAC'02

Avoiding negative steps & decreasing the number of terms to evaluate

$\mathcal{SABA}$ and $\mathcal{SBAB}$ Classes

Let us split the Hamiltonian into two parts A et B, **symmetric symplectic integrators** can be obtained from one of the **two classes** $\mathcal{SABA}_k$ and $\mathcal{SBAB}_k$:

$$\begin{aligned}
\mathcal{SABA}_{2n} &: e^{c_1 s L_A} e^{d_1 s L_{\epsilon B}} \dots e^{d_n s L_{\epsilon B}} e^{c_{n+1} s L_A} e^{d_n s L_{\epsilon B}} \dots e^{d_1 s L_{\epsilon B}} e^{c_1 s L_A} \\
\mathcal{SABA}_{2n+1} &: e^{c_1 s L_A} e^{d_1 s L_{\epsilon B}} \dots e^{c_{n+1} s L_A} e^{d_{n+1} s L_{\epsilon B}} e^{c_{n+1} s L_A} \dots e^{d_1 s L_{\epsilon B}} e^{c_1 s L_A} \qquad (26) \\
\mathcal{SBAB}_{2n} &: e^{d_1 s L_{\epsilon B}} e^{c_2 s L_A} e^{d_2 s L_{\epsilon B}} \dots e^{d_n s L_{\epsilon B}} e^{c_{n+1} s L_A} e^{d_n s L_{\epsilon B}} \dots e^{d_2 s L_{\epsilon B}} e^{c_2 s L_A} e^{d_1 s L_{\epsilon B}} \\
\mathcal{SBAB}_{2n+1} &: e^{d_1 s L_{\epsilon B}} e^{c_2 s L_A} e^{d_2 s L_{\epsilon B}} \dots e^{c_{n+1} s L_A} e^{d_{n+1} s L_{\epsilon B}} e^{c_{n+1} s L_A} \dots e^{d_2 s L_{\epsilon B}} e^{c_2 s L_A} e^{d_1 s}
\end{aligned}$$

NB: k is the number of evaluations of $e^{c_k s L_A}$ ($e^{d_k s L_{\epsilon B}}$) operators.

Laskar, J., Robutel, P.: *High order symplectic integrators for perturbed Hamiltonian systems*, Celestial Mechanics and Dynamical Astronomy, Vol. 80, No. 1., pp. 39–62.

Particle beam dynamics optimization

FREQUENCY MAP ANALYSIS

Frequency Map Analysis
Laskar A&A1988, Icarus1990

Numerical **A**nalysis of **F**undamental **F**requency

Quasi-periodic approximation through **NAFF** algorithm $f'_j(t) = \sum_{k=1}^{N} a_{j,k} e^{i\omega_{j,k} t}$

of a complex phase space function $f_j(t) = q_j(t) + i p_j(t)$

defined over $t = \tau,$

for each degree of freedom $j = 1, \ldots, n$ with $\omega_{j,k} = \boldsymbol{k}_j \cdot \boldsymbol{\omega}$

and $a_{j,k} = A_{j,k} e^{i\phi_{j,k}}$

Frequency Map Analysis

Laskar A&A1988, Icarus1990 NATO-ASI 1996

- Construction of frequency map

$$\mathcal{F}_\tau : \begin{array}{ccc} \mathbb{R}^n & \longrightarrow & \mathbb{R}^n \\ q|_{p=p_0} & \longrightarrow & \boldsymbol{\nu} \end{array}$$

- Determination of tune diffusion vector

$$\boldsymbol{D}|_{t=\tau} = \boldsymbol{\nu}|_{t\in(0,\tau/2]} - \boldsymbol{\nu}|_{t\in(\tau/2,\tau]}$$

and construction of diffusion map

with high precision: $\dfrac{1}{\tau^4}$ for Hanning Filter

$$\mathcal{D}_\tau : \begin{array}{ccc} \mathbb{R}^n & \longrightarrow & \mathbb{R}^n \\ q|_{p=p_0} & \longrightarrow & \boldsymbol{D} \end{array}$$

- Refined Fourier technique
- Fast convergence (reduce tracking time)
- Give a global view of the transverse dynamics in a 2D map
- Mapping between DA/tune space using diffusion index

Does not direct provide a way to optimize
But is a figure of Merit

- Determination of resonance driving terms associated with amplitudes $a_{j,k}$

Bengtsson PhD thesis CERN88-05

Turn by turn (TbT)data beam smearing

- **TbT BPM precision**: 10µm ~10 mA: limitative factor Frequency shift
- Algo. to precisely determine tune loose their precision *R. Bartolini et al. Part. Acc. 55, 247 (1995)*
- Lines excited by resonance of order (m+1) decohere m times faster than the tune line. *R. Thomas, PHd Thesis (2003)*
- Gain, coupling correction (LOCO based)

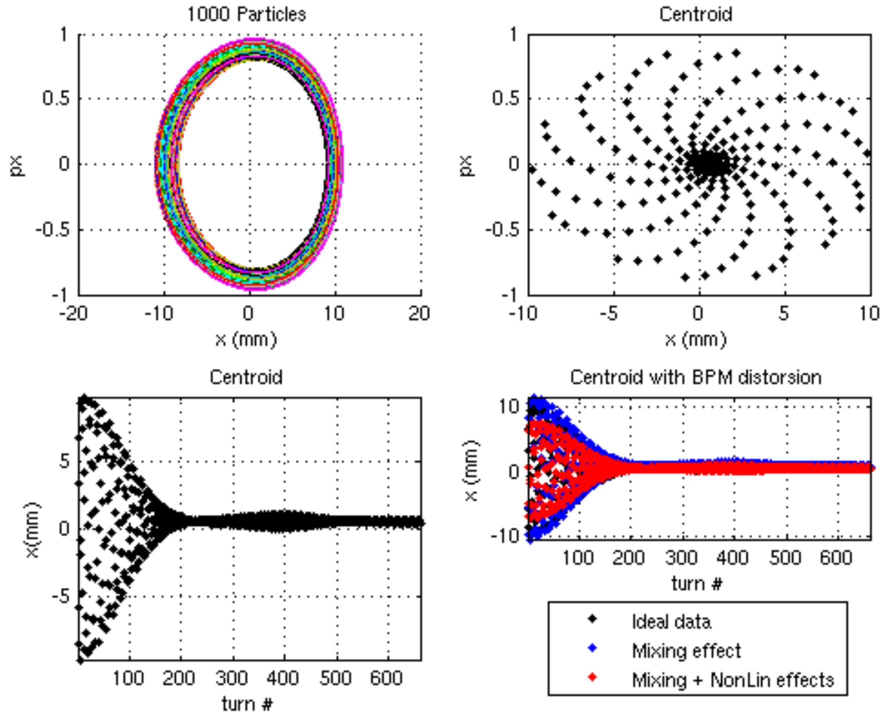

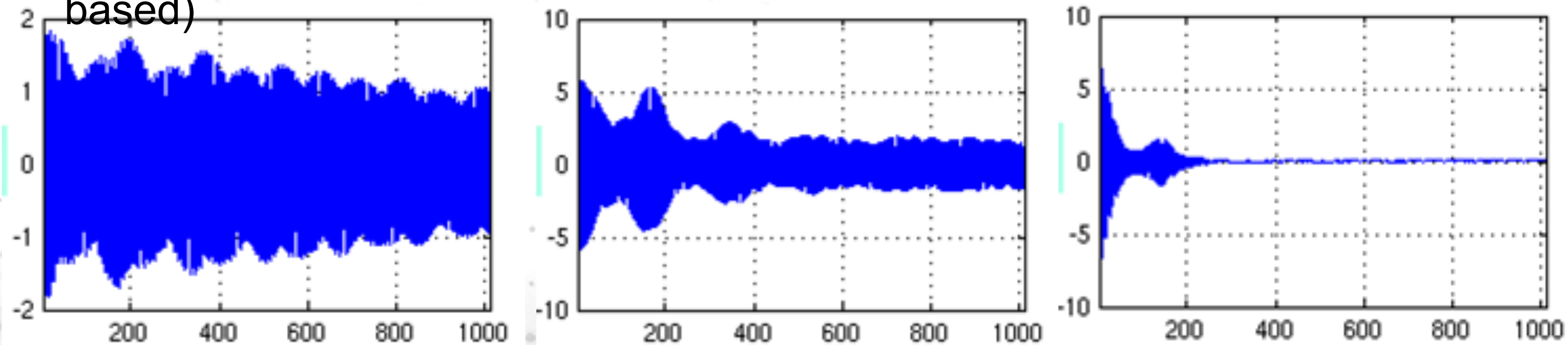

V (kicker H) : 2100 V 9000 V 12100 V

x (BPM) : 3.6 mm 15.2 mm 20.6 mm

Accelerator 4D Dynamics

A particle $\Longrightarrow$ 3 degrees of freedom

$$
\begin{aligned}
F^T : \mathbb{R}^2 &\quad\rightarrow\quad \mathbb{R}^2 \\
(x,\ y) &\quad\mapsto\quad (\nu_x,\ \nu_y)
\end{aligned}
$$

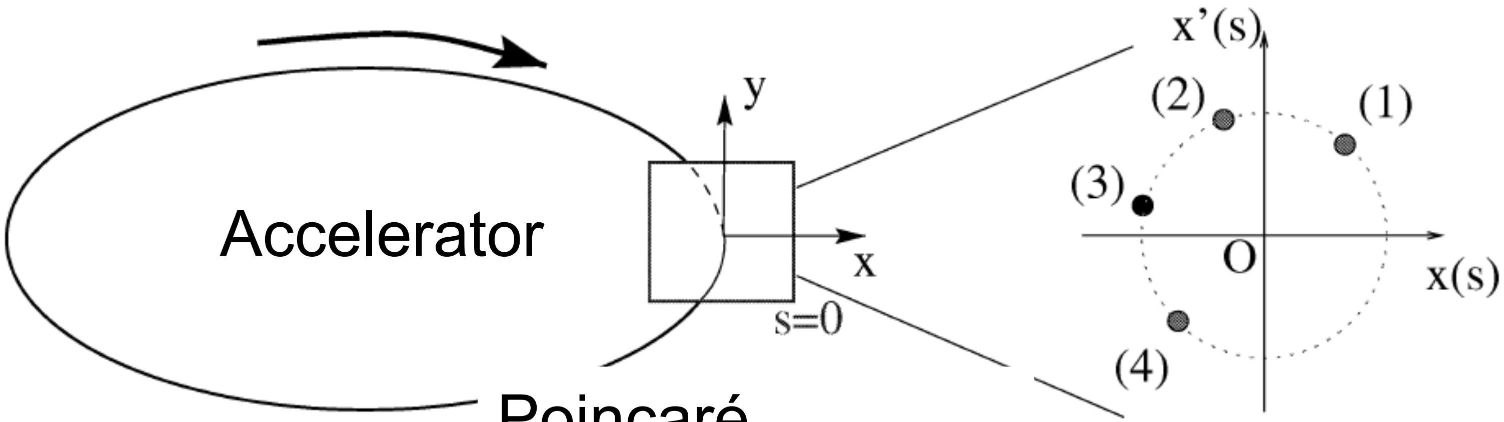

Poincaré
Surface of section

Computing a frequency map

Frequency map: $F^T : (x_0,z_0) \longrightarrow (\nu_x,\nu_z)$

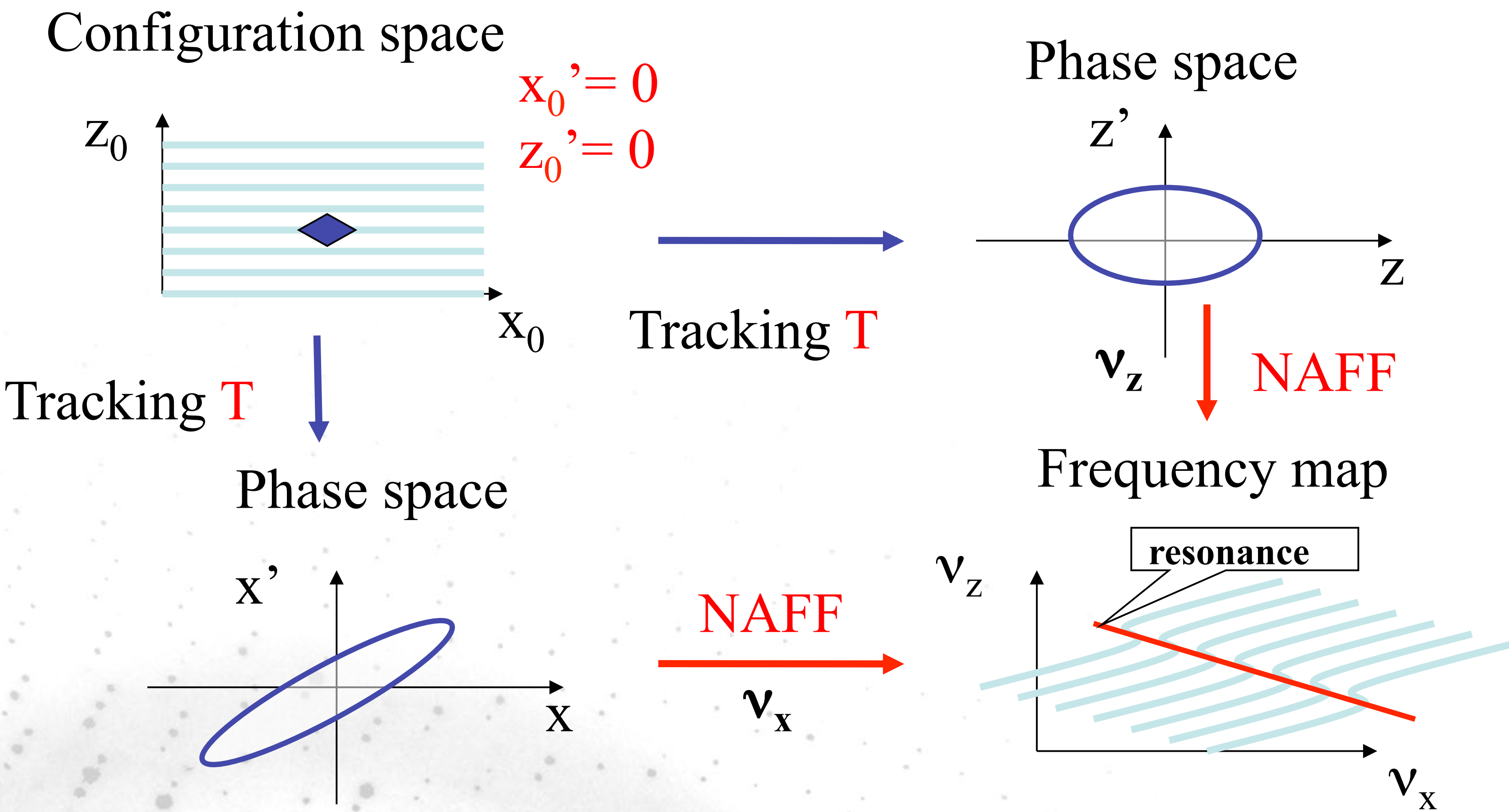

Reading a FMA

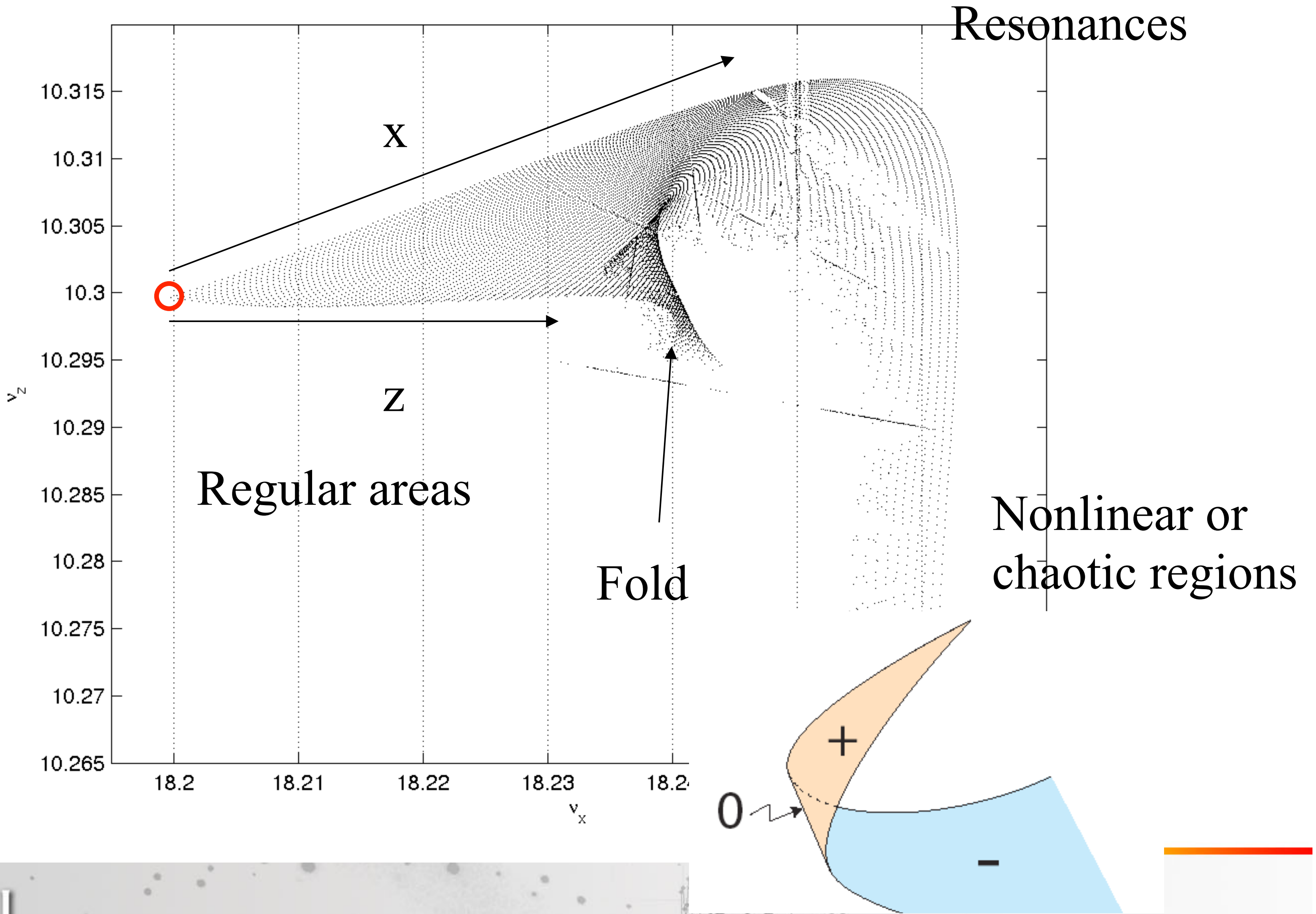

Resonance network: $a\,\nu_x + b\,\nu_z = c$

order = |a| + |b|

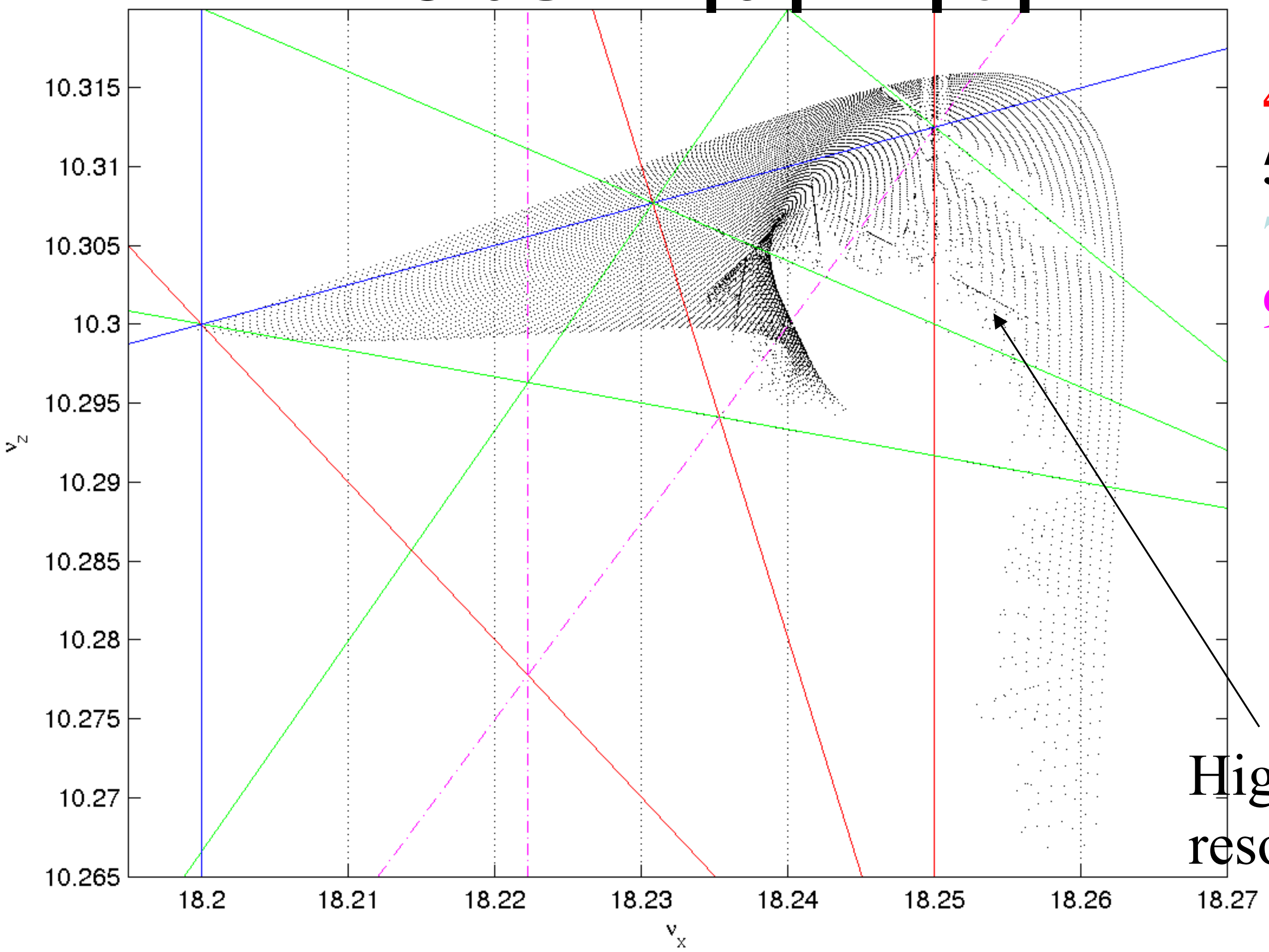

4th order
5th order
7th order
9th order

Higher order resonance

Diffusion $D = (1/N)*\log10(||Dn||)$

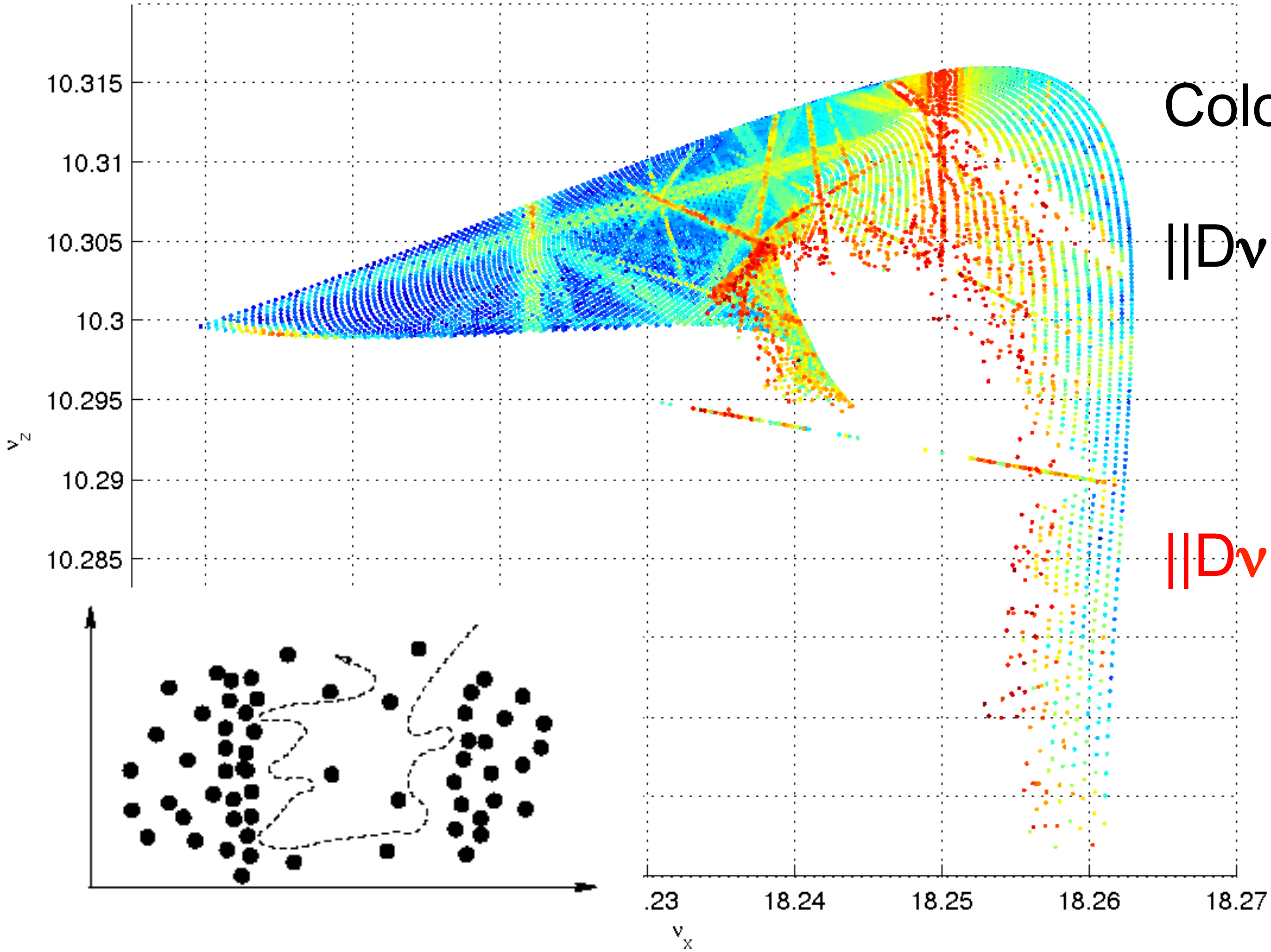

Color code:

$||D\nu|| < 10^{-10}$

$||D\nu|| > 10^{-2}$

Diffusion reveals as well slightly excited resonances

On-momentum Dynamics --Working point: (18.2,10.3)

Bare lattice (no errors)

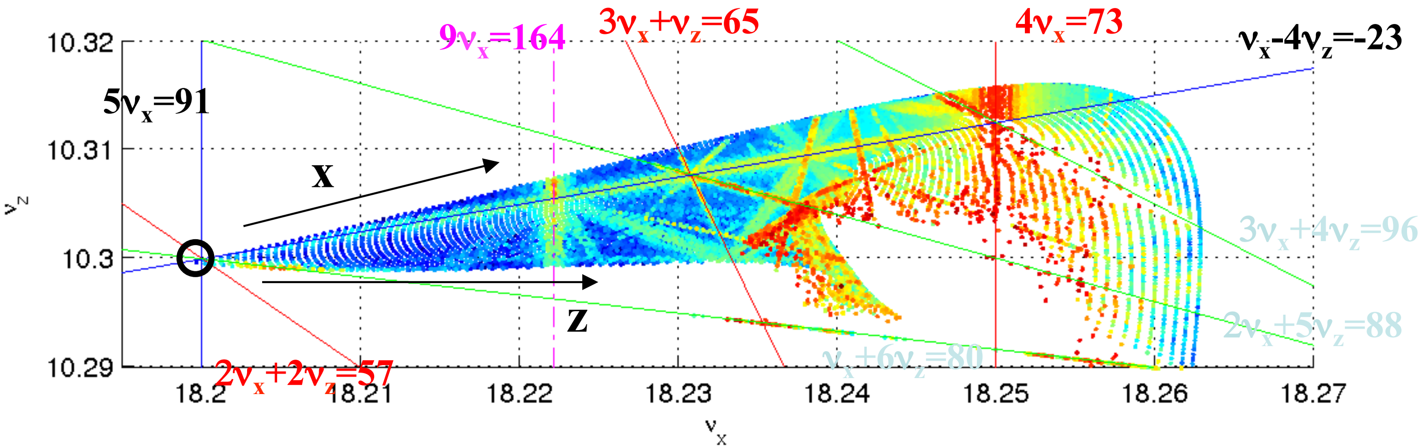

WP sitting on

Resonance node

$\nu_x + 6\nu_z = 80$

$5\nu_x = 91$

$\nu_x - 4\nu_z = -23$

$2\nu_x + 2\nu_z = 57$

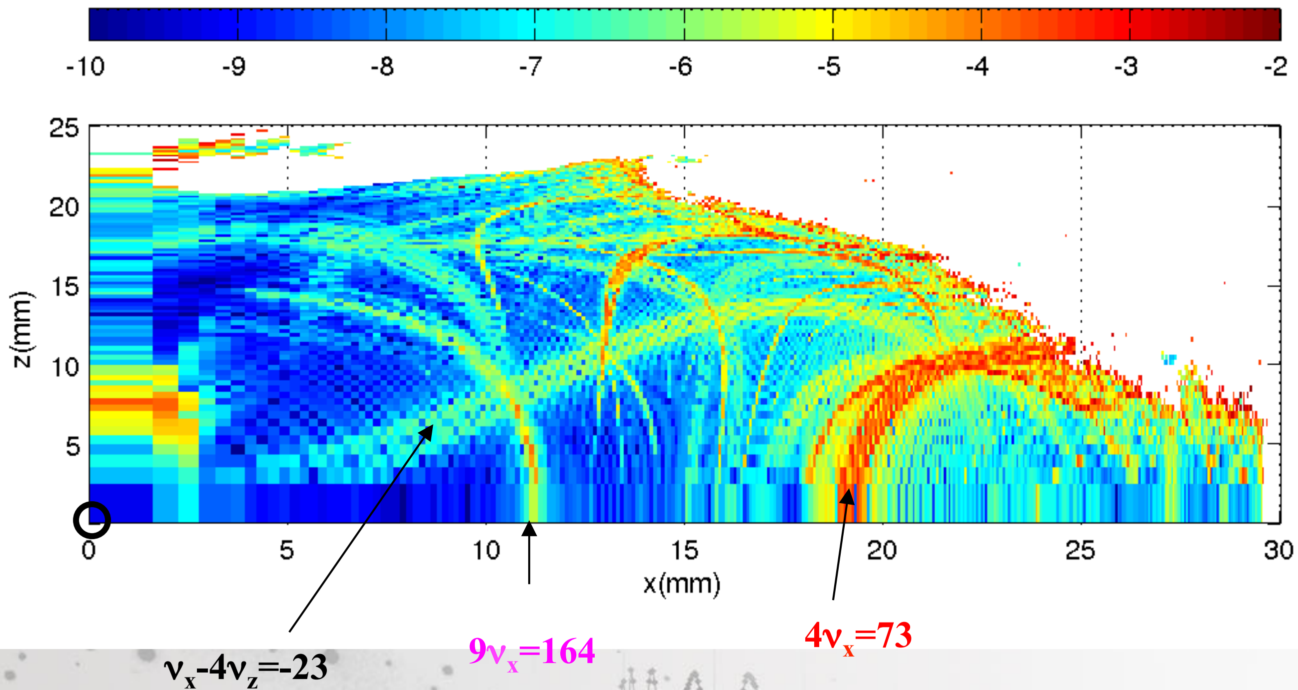

On-momentum dynamics w/ 1.9% coupling (18.2,10.3)

Randomly rotating 160 Quads

- **Map fold is destroyed**
- **Coupling strongly impacts**

$3\nu_x + \nu_z = 65$

- **Resonance node excited**

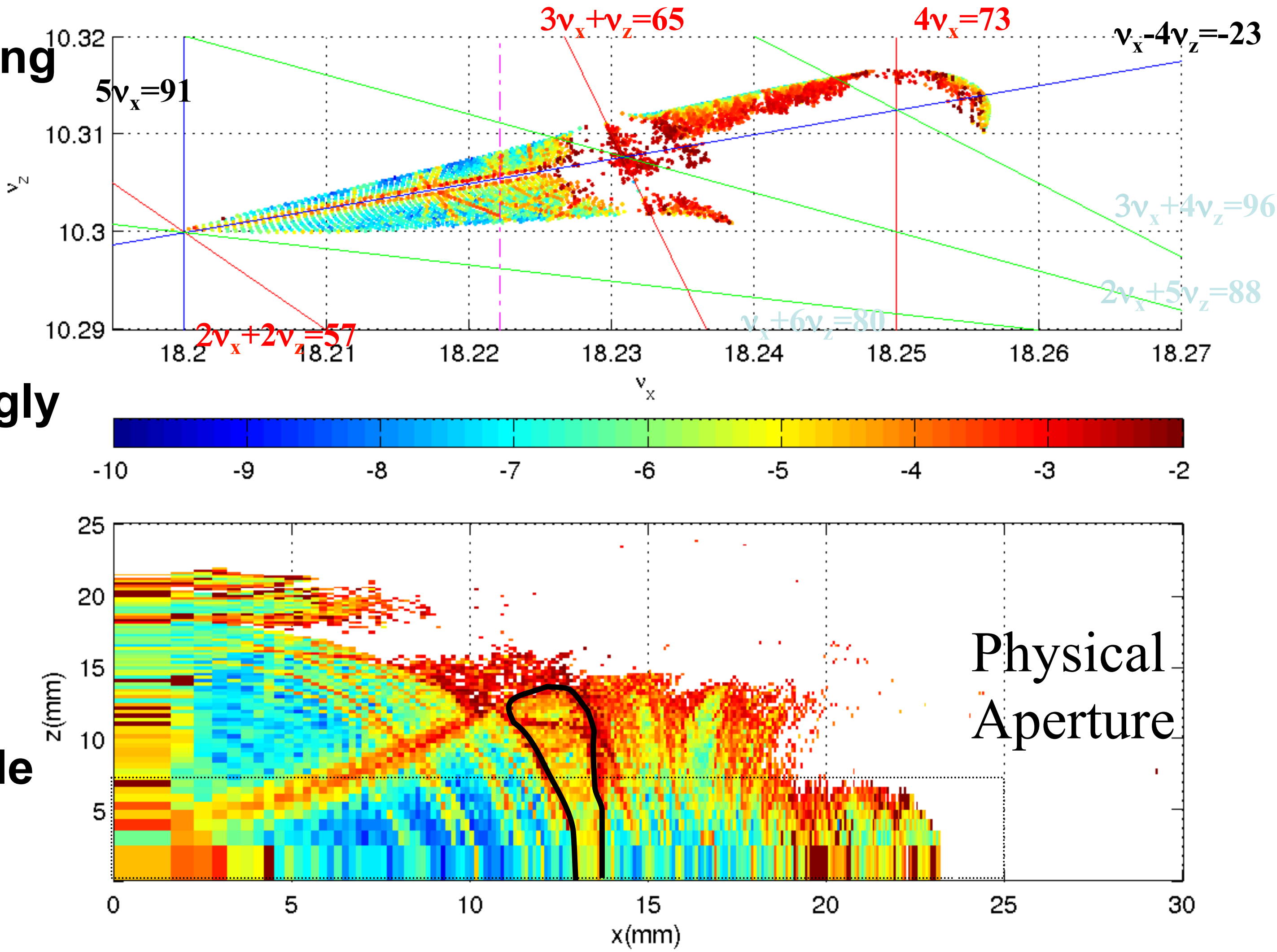

Resonance island $3\nu_x+\nu_z=65$

Frequency Map Analysis: ALS and BESSY-II

P. Kuske (BESSY-II)

ALS linear lattice corrected to 0.5% rms β-beating

FM computed including residual β-beating and coupling errors

BESSY-II with harmonic sextupole magnets, chromaticity, coupling

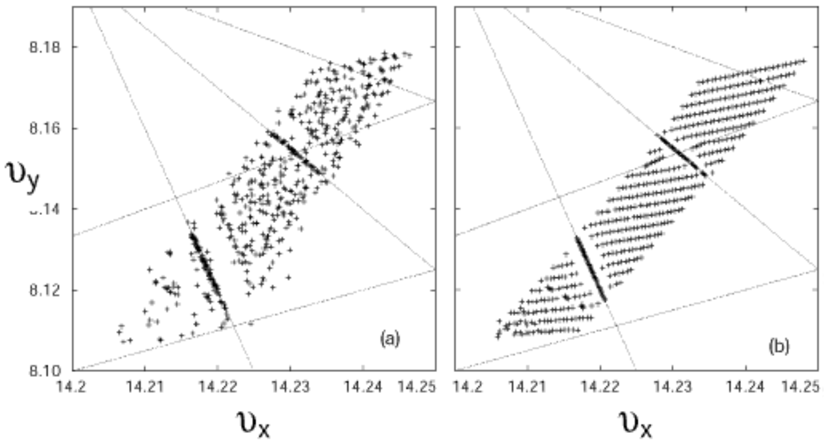

ALS measured ALS model

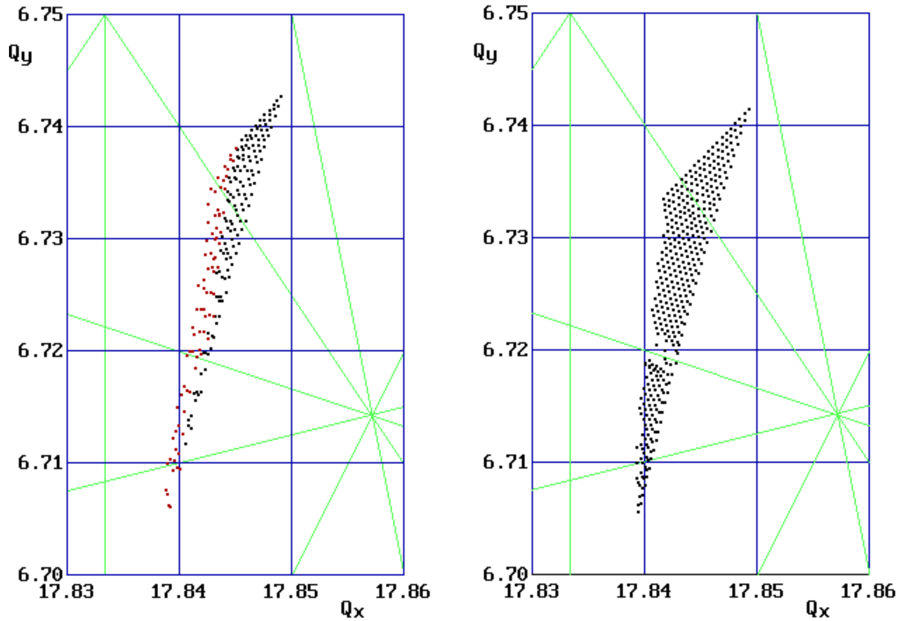

BESSY-II measured BESSY-II model

D. Robin et al PRL 85, 3 (2000)

A very accurate description of machine model is mandatory

- fringe fields: dipole, quadrupole (and sextupole) magnets
- systematic octupole components in quadrupole magnets
- decapoles, skew decapoles and octupoles in sextupole magnets

Courtesy C. Steier (ALS) P. Kuske (BESSY-II)

Off-momentum dynamics: beam lifetime

Several approaches:

- **Off-momentum frequency maps**
- **Energy/betatron-amplitude frequency maps**
- **Touschek lifetime**
  - 4D tracking
  - 6D tracking

Particle behavior after Touschek scattering

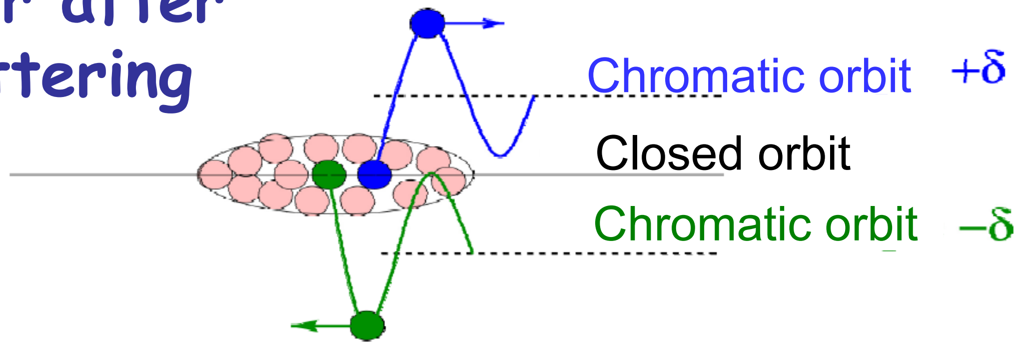

$$x = \sqrt{A_x \beta_{x_1}} + \eta_0 \delta$$

$$A_x = \gamma_{x_0} (\eta_0 \delta)^2 + 2 \alpha_{x0} (\eta_0 \delta)(\eta_0' \delta) + \beta_{x0} (\eta_0' \delta)^2$$

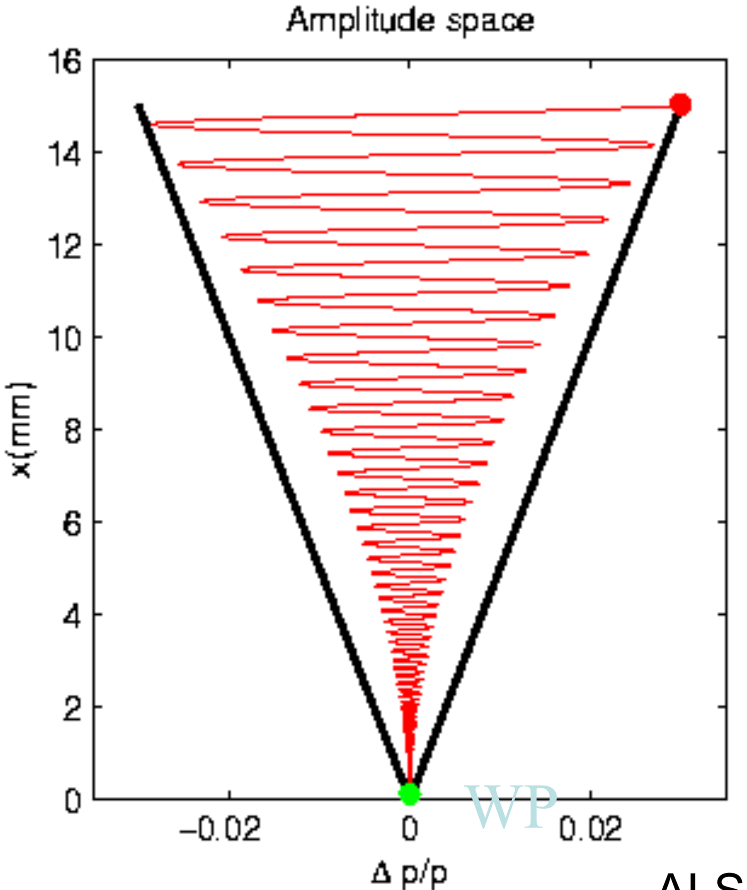

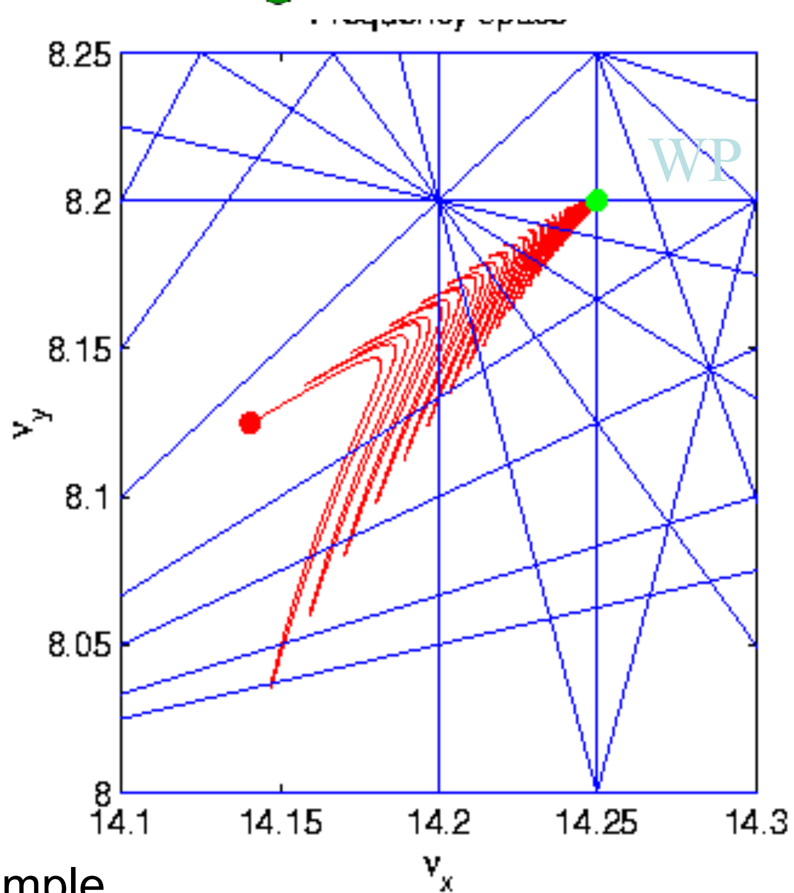

ALS Example

Off momentum dynamics

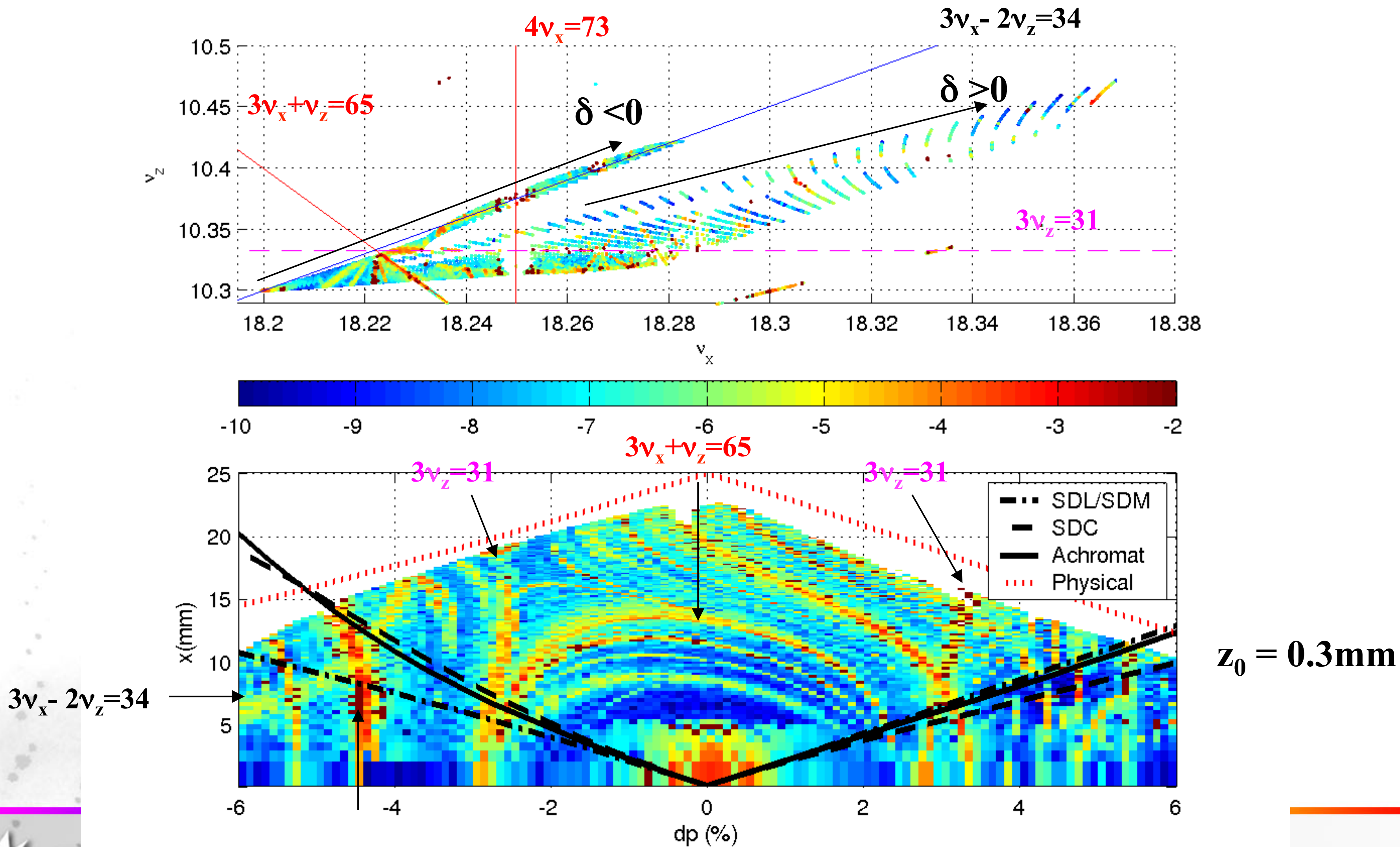

The SOLEIL energy acceptance of the bare machine is large : +/- 4%.

Agreement of a few percents (a factor 2 common 20 year ago)

Complete optimized linear and non-linear model

Simulations

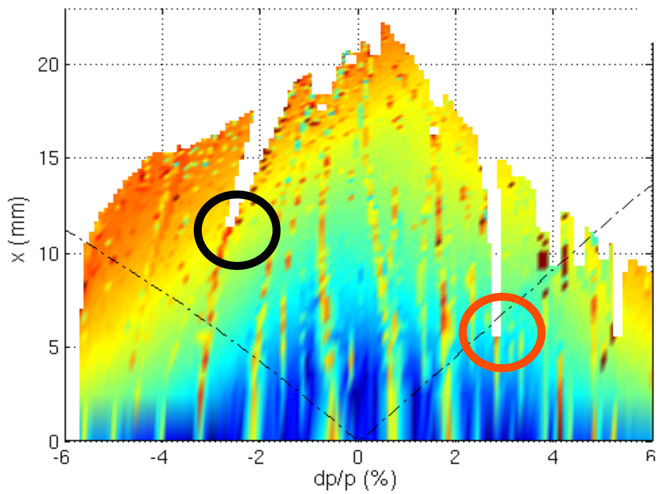

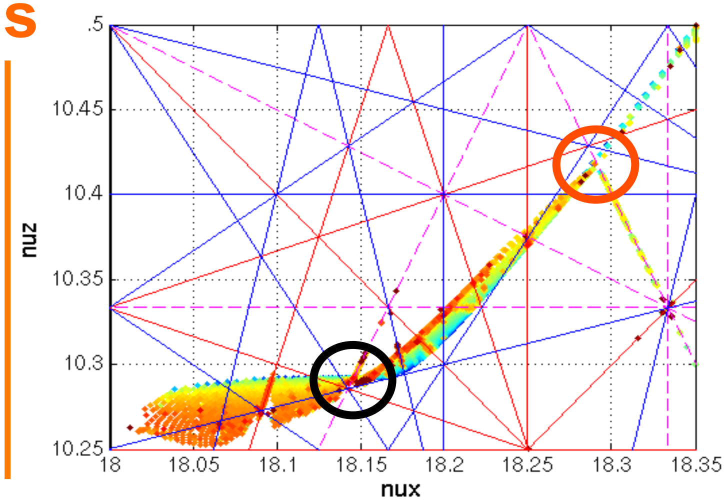

- dp/p = + 4 % : $3\nu_x=55.$
- dp/p = + 3 % : $2\nu_x+\nu_z=47$
- dp/p = - 3 % : $2\nu_x-\nu_z=26$

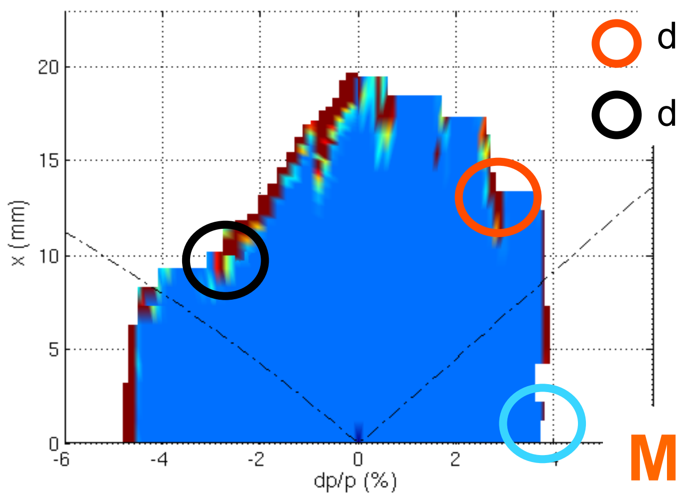

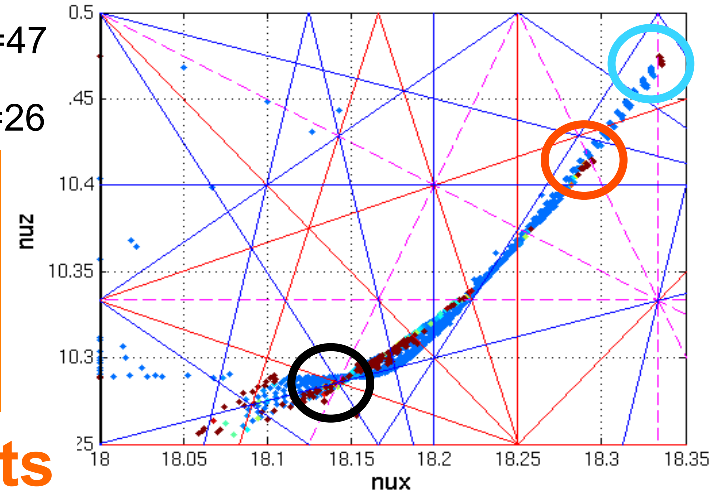

Measurements

P. Brunelle et al, IPAC

LASKAR'S LEGACY TO THE ACCELERATOR COMMUNITY

Existing 3rd Generation Light Sources

1992	**ESRF**, France (EU)	6 GeV
1993	**ALS**, USA	1.5-1.9 GeV
	TLS, Taiwan	1.5 GeV
1994	**ELETTRA**, Italy	2.4 GeV
	PLS, Korea	2 GeV
	MAX II, Sweden	1.5 GeV
1996	**APS**, USA	7 GeV
	LNLS, Brazil	1.35 GeV
1997	**Spring-8**, Japan	8 GeV
1998	**BESSY II**, Germany	1.9 GeV
2000	**ANKA**, Germany	2.5 GeV
	SLS, Switzerland	2.4 GeV
2004	**SPEAR3**, US	3 GeV
	CLS, Canada	2.9 GeV
2006	**SOLEIL**, France	2.75 GeV
	DIAMOND, UK	3 GeV
	ASP, Australia	3 GeV
	MAX III, Sweden	700 MeV
	Indus-II, India	2.5 GeV
2008	**SSRF**, China	3.5 GeV
2009	**PETRAIII, **Germany	6.0 GeV
2011	**ALBA, **Spain	3.0 GeV

3rd GLS under construction or planned

Under construction

End 2014	**NSLS-II**, US	3 GeV
2015	**MAX-IV**, Sweden	3 GeV
2015	**SOLARIS**, Poland	1.5 GeV
2015	**TPS**, Taiwan	3 GeV
2016	**SESAME**, Jordan	2.5 GeV
2016	**SIRIUS**, Brazil	3 GeV

Upgrade foreseen for most of the present light sources (ALS, DIAMOND, SOLEIL, …)

CANDLE, Armenia	3 GeV
ILSF, Iran	3 GeV
BAPS, China	5 GeV
Another Japanese	3 GeV
PEP-X, US	4.5 GeV,
5-10 pm.	
tUSR, US	9 GeV
Russian	3 GeV,
HALS, China	1.5 GeV

Simple to complex facilities

D. Robin et al. / Nuclear Instruments and Methods in Physics Research A 538 (2005) 65–92

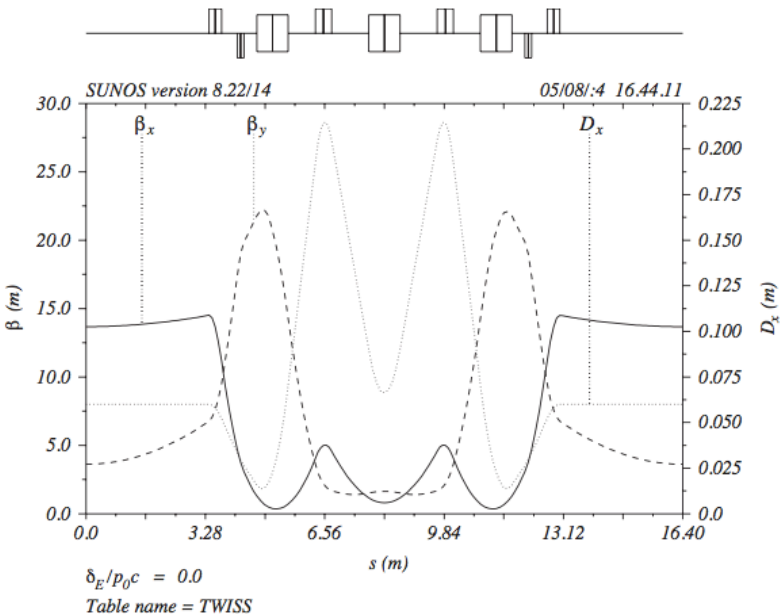

Fig. 4. Lattice functions (β_x, β_y, η_x) of the ALS for the zero dispersion lattice used before Superbends were installed.

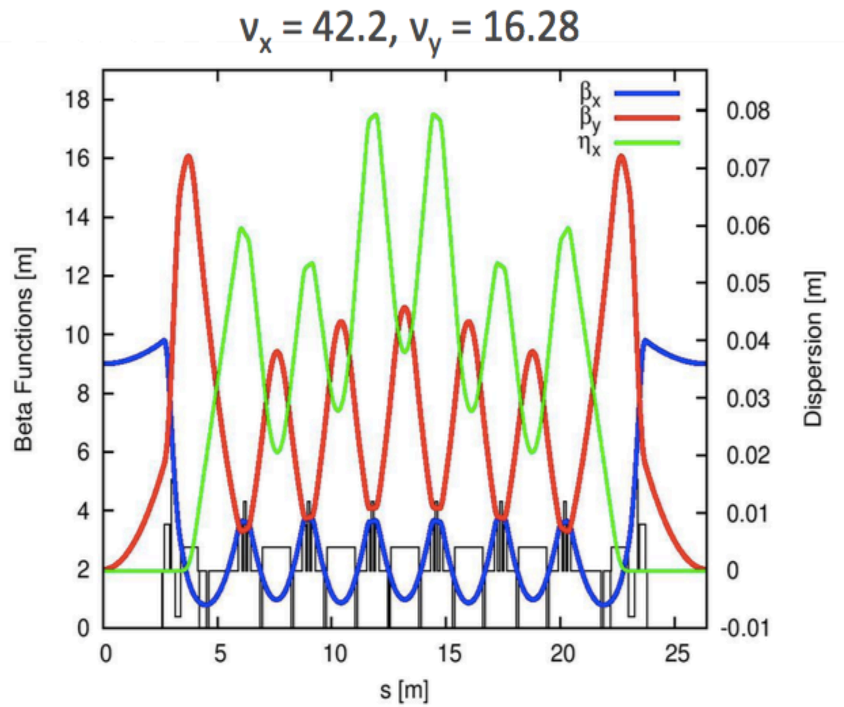

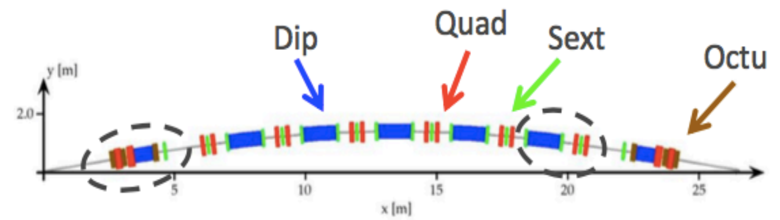

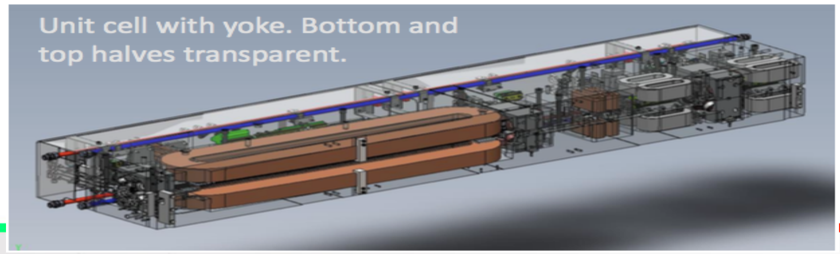

Simple lattice with **2 independent families** of sextupole magnets to lattices with many familites or individual of sextupoles, n-poles (octupole, …) → strong nonlinarities

Examples of use of FMA
For optimizing circular accelerators

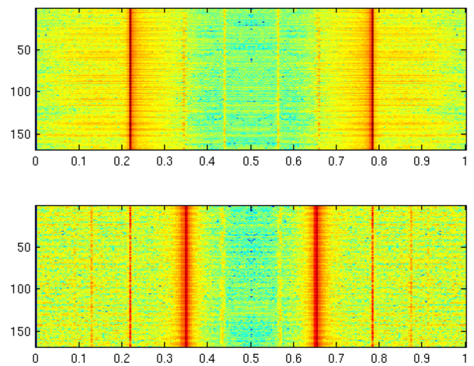

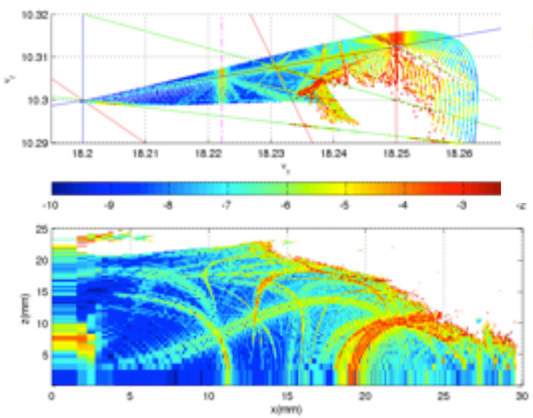

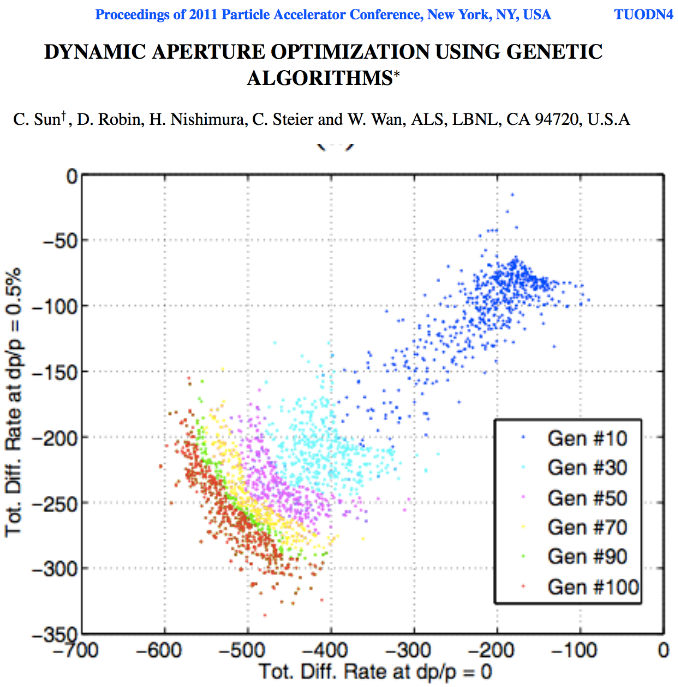
Proceedings of 2011 Particle Accelerator Conference, New York, NY, USA TUODN4

DYNAMIC APERTURE OPTIMIZATION USING GENETIC ALGORITHMS*

C. Sun†, D. Robin, H. Nishimura, C. Steier and W. Wan, ALS, LBNL, CA 94720, U.S.A

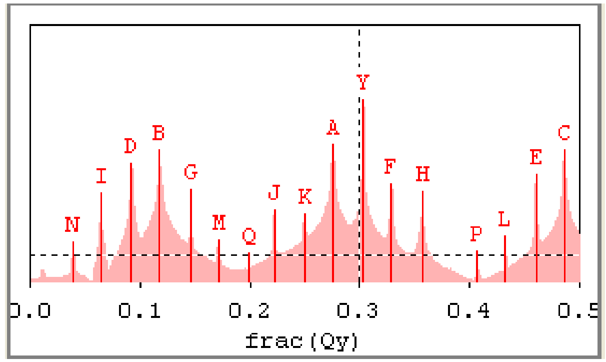

Courtesy of R. Bartolini

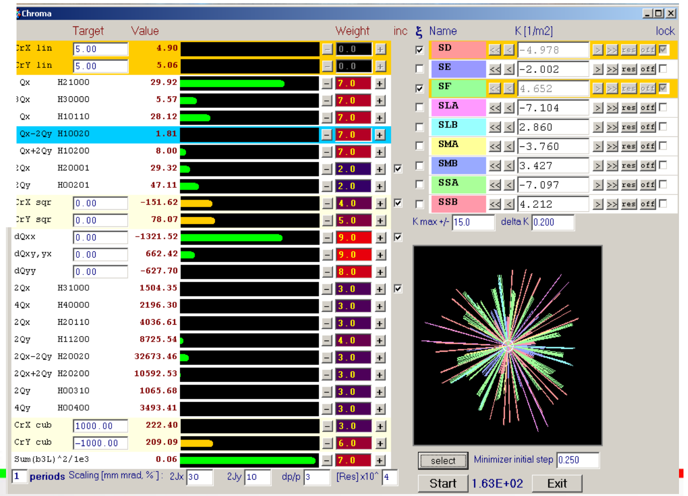

Genetic algorithm based optimization
Diffusion rate

Conclusions of more than 15 years of Frequency Map Analysis

FMA techniques used in all facilities
Standard tool of any accelerator physicist

- Gives us a global view (footprint of the dynamics) : a 2D map
- Reveals the dynamics sensitivity to magnet errors, coupling errors, alignement errors, sextupoles and insertion devices…
- Reveals nicely effect of coupled resonances, specially cross term $\nu_z(x)$
- Enables us to modify the working point to avoid resonances or regions in frequency space
- Is suitable both for simulation and online data
- Benchmarking models and beam-based dynamics

Thank you Jacques for your contribution

Pioneer work at ALS
see talk by D. Robin

FMA workshop 2002 (IMCCE)
FMA workshop 2004 (LURE)
…

Accelerator community